

LCODE user manual

K.V. Lotov, A.P. Sosedkin

December 7, 2023

Contents

1	Overview	2
2	Notation and units of measure	3
3	Underlying physics	6
3.1	Kinetic plasma model	6
3.2	Fluid plasma model	7
3.3	Beam model	8
3.4	Energy fluxes and energy densities	9
3.5	Laser beams	9
4	Running the code	10
4.1	Overview	10
4.2	Input files	10
4.3	Configuration options and files	11
4.4	Interactive control	12
4.5	Exit codes	12
4.6	Parallel calculations with the MPI-enabled version	12
5	Configuration file	12
5.1	Simulation area	13
5.2	Particle beams	13
5.2.1	Newly generated beams	14
5.3	Laser beams	15
5.3.1	Self-consistent evolution of the laser beam	15
5.4	Plasma	16
5.4.1	Options specific to particle plasma models	16
5.4.2	Option specific to the fluid plasma model	18
5.5	Every-time-step diagnostics	18
5.6	Periodical diagnostics	19
5.6.1	Colored maps	19
5.6.2	Functions of ξ	22
5.6.3	Beam particle information as pictures	24
5.6.4	Beam information as histograms	24
5.6.5	Trajectories of plasma particles	25
5.6.6	Detailed (substepped) plasma response	26
5.7	Saving run state	27
5.8	Performance	27
5.9	Logging preferences	27
5.10	Miscellaneous options	28
6	Initial beam shape	28
6.1	Segment parameters	28
6.2	Example of a beam profile	30

7	Format of other input and output files	30
7.1	beamfile.bin	30
7.2	beamfile.bit	31
7.3	plasma.bin	31
7.4	fields.bin	31
7.5	Laser files ls?????.???swp	31
7.6	r*****.det	31
7.7	times.dat	32
7.8	Diagnostics files	32
7.9	Temporary files	32
8	Tools built into LCODE	32
8.1	Beamfile composition/manipulation	32
8.2	Beamfile inspection	33

1 Overview

LCODE is a freely-distributed code for simulations of particle beam-driven plasma wakefield acceleration. The code is 2-dimensional (2d3v), with both plane and axisymmetric geometries possible. In the code, the simulation window moves with the light velocity, and the quasi-static approximation is used for calculating plasma response. The beams are modeled by fully relativistic macro-particles. The plasma is modeled either by macro-particles (kinetic solver), or as the electron fluid (fluid solver). Transversely inhomogeneous plasmas, hot plasmas, non-neutral plasmas, and mobile ions are possible with the kinetic solver. The code is furnished with extensive diagnosing tools which include the possibility of in-flight graphical presentation of the results.

The essence of the quasi-static approximation is illustrated by Figure 1. When we calculate the plasma response, the beam is considered as a “rigid” (not evolving in time) distribution of charges and currents which propagates with the speed of light c . The fields generated by this beam depend on the longitudinal coordinate z and time t only in combination $\xi = z - ct$ and can be found layer-by-layer starting from the beam head. Since the beam is not changing, all particles started from some transverse position r_0 copy the motion of each other, and their parameters (transverse coordinate and momenta) can be found as functions of ξ . Thus, a plasma macroparticle in the quasi-static model is not a “big” particle, but a “particle tube,” i.e., a group of real particles started from a given radius with a given initial momentum. This greatly reduces the memory required for storing plasma particles.

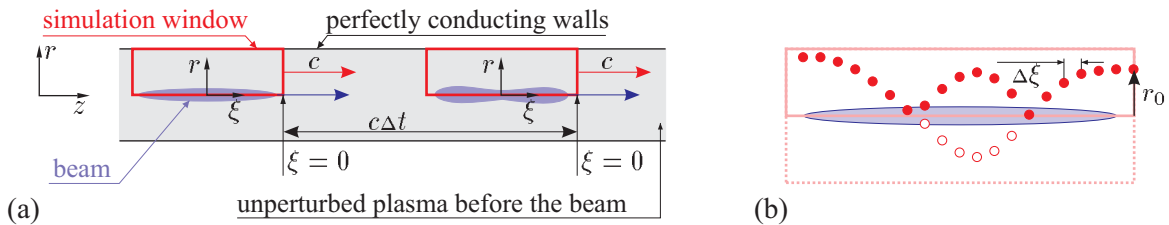


Figure 1: Geometry of the problem (a), and trajectory of a plasma particle in the simulation window (b).

The calculated fields are then used to modify the beam. For highly relativistic beams, the time step Δt for beam particles can be made large, which speeds up simulations several orders of magnitude. The quasi-static approximation is thus useful if and only if the time scale of beam evolution is much longer than the period of plasma wave.

Various details of LCODE and underlying physics are described in the following papers:

- K.V. Lotov, *Simulation of ultrarelativistic beam dynamics in plasma wake-field accelerator*. Phys. Plasmas **5**, 785 (1998). — The fluid plasma model.
- K.V. Lotov, *Fine wakefield structure in the blowout regime of plasma wakefield accelerators*. Phys. Rev. ST - Accel. Beams **6**, 061301 (2003). — The beam model and the kinetic plasma model.
- K.V. Lotov, *Blowout regimes of plasma wakefield acceleration*. Phys. Rev. E **69**, 046405 (2004). — Energy fluxes in the co-propagating window.

- K.V. Lotov, V.I. Maslov, I.N. Onishchenko, and E.N. Svistun, *Resonant excitation of plasma wakefields by a non-resonant train of short electron bunches*. Plasma Phys. Control. Fusion **52**, 065009 (2010). — Discussion on applicability of quasi-static codes to simulations of long beams.
- K.V. Lotov, A. Sosedkin, E. Mesyats, *Simulation of Self-modulating Particle Beams in Plasma Wakefield Accelerators*. Proceedings of IPAC2013 (Shanghai, China), p.1238-1240. — Upgrade of the kinetic plasma solver which was necessary for simulations of long beams.
- A.P. Sosedkin, K.V. Lotov, *LCODE: A parallel quasistatic code for computationally heavy problems of plasma wakefield acceleration*. Nuclear Instr. Methods A **829**, 350 (2016). — Parallelization.
- R.N. Spitsyn, *Numerical realization of quasistatic model of laser driver for plasma wakefield acceleration* (in Russian). Master theses, Novosibirsk State University (2016).

2 Notation and units of measure

We use cylindrical coordinates (r, φ, ξ) for the axisymmetric geometry and Cartesian coordinates (x, y, ξ) for the plane geometry. The beam propagates in positive ξ -direction.

The code works with dimensionless quantities. Units of measure depend on some basic plasma density n_0 . It is recommended to use the initial unperturbed plasma density as n_0 . All times are in units of ω_p^{-1} , where $\omega_p = \sqrt{4\pi n_0 e^2 / m}$ is the electron plasma frequency, e is the elementary charge, and m is the electron mass. All distances are in units of c/ω_p . The unit velocity is c . The notation used and units of measure for various quantities are given in Table 1.

Table 1: Notation, units of measure, and places of first appearance or definition for various quantities.

Notation	Quantity & place of definition	Unit
Times:		ω_p^{-1}
t	Time in general (Sec. 1) or propagation time for the beam	
Δt	Main time step for the beam, Sec. 1, Sec. 5.1, time-step	
$\Delta t'$	Reduced time step for the beam, Sec. 5.1, beam-substepping-energy	
t_{\max}	Time limit for the run, Sec. 5.1, time-limit	
t_F	Period of the external beam focusing, Sec. 5.2, foc-period	
t_B	Oscillation period for the external magnetic field, Sec. 5.4, magnetic-field-period	
Δt_{out}	Periodicity of the detailed output, Sec. 5.6, output-time-period	
Frequencies:		ω_p
ω_0	Laser frequency, Sec. 3.5, laser-wavenumber	
Lengths:		c/ω_p
ξ	The co-moving coordinate, Sec. 1	
$\Delta \xi$	Longitudinal grid step, Sec. 3.1, Sec. 5.1, xi-step	
$\vec{r}_b, r_b, x_b, \xi_b$	Coordinates of a beam macro-particle, Sec. 3.3	
σ_{rl}, σ_{r0}	Transverse sizes of the laser pulse, Sec. 3.5	
σ_{zl}, L_l	Longitudinal sizes of the laser pulse, Sec. 3.5	
ξ_c, ξ_{i0}	Longitudinal positions of the laser pulse center (current and initial), Sec. 3.5	
x_l	Initial transverse position of the laser pulse center, Sec. 3.5	
Z_r	Rayleigh length, Sec. 3.5	
ξ_{\max}	Length of the simulation window, Sec. 5.1, window-length	
Δr	Transverse grid step, Sec. 5.1, r-step	
r_{\max}	Transverse size of the simulation window, Sec. 5.1, window-width	
r_p, r_{p2}	Width parameters for some plasma density profiles, Sec. 5.4.1, plasma-profile	
l_p, l_{p0}, l_m, P	Segment length, position where the segment begins and where the density is calculated, and (sometimes) additional parameter of the segment, if the plasma density varies in z , Sec. 5.4.1, plasma-zshape	
L_{trap}	Path limit for trapped plasma particles, Sec. 5.4.1, trapped-path-limit	
X_{b0}	Transverse displacement of the beam slice, Sec. 5.6.2, f(xi)	
R_b, X_b	Radius or half-width of the beam slice, Sec. 5.6.2, f(xi)	
ϵ	Emittance of the beam slice, Sec. 5.6.2, f(xi)	
$\xi_{\text{from}}, \xi_{\text{to}}$	Left and right boundaries of the subwindow, Sec. 5.6.1, subwindow-xi-from	

$r_{\text{from}}, r_{\text{to}}$	Bottom and top boundaries of the subwindow, Sec. 5.6.1, subwindow-xi-from
$r_{\text{ax}}, r_{\text{aux}}$	Two transverse coordinates to output functions of ξ at, Sec. 5.6.2, axis-radius
l_s	Length of the beam segment, Sec. 6.1, length
$\delta\xi$	Distance to beginning of the beam segment, Sec. 6.1, xishape
ξ_s	ξ -coordinate the segment begins at ($\xi_s < 0$), Sec. 6.1, xishape
σ_r	Transverse size of the beam segment, Sec. 6.1, xishape
σ_z	Length parameter for the Gaussian beam segment, Sec. 6.1, xishape
x_0	Transverse displacement of the segment, Sec. 6.1, vshift
Velocities: c	
\vec{v}	Velocity of a plasma macro-particle or of an electron fluid element, Sec. 3.1, Sec. 3.2
\vec{v}_i	Velocity of i -th plasma macro-particle, Sec. 3.1
\vec{v}_b	Velocity of a beam macro-particle, Sec. 3.3
Momenta: mc	
\vec{p}	Momentum of a plasma macro-particle or of an electron fluid element, Sec. 3.1, Sec. 3.2
\vec{p}_b	Momentum of a beam particle (not of a heavy macro-particle), Sec. 3.3
Δp_{foc}	Extra momentum gained by a beam particle due to external focusing, Sec. 5.2, focusing
\vec{p}_e	Momentum of a plasma electron, Sec. 5.6.1, colormaps-full
\vec{p}_i	Momentum of a plasma ion, Sec. 5.6.1, colormaps-full
$p_{b,\text{ref}}$	Reference value for displaying beam momentum, Sec. 5.6.4, output-reference-energy
p_{b0}	Basic longitudinal momentum of beam particles in the segment, Sec. 6.1, energy
p_a	Auxiliary value of the longitudinal momentum for the beam segment, Sec. 6.1, espread
Angular momentum: mc^2/ω_p	
M_b	Angular momentum of a beam particle, Sec. 7.1
Masses: m	
M	Mass of a plasma macro-particle, Sec. 3.1
m_b	Mass of a beam particle, Sec. 3.3
M_p	Mass of a plasma particle, Sec. 3.5
Number densities: n_0	
n_e	Density of plasma electrons, Sec. 3.2, Sec. 5.6.1, colormaps-full
n_i	Density of plasma ions, Sec. 3.2, Sec. 5.6.1, colormaps-full
$n(r)$	Initial transverse profile of the plasma density, Sec. 5.4.1, plasma-profile
n_{p2}	A parameter for some plasma density profiles, Sec. 5.4.1, plasma-profile
Charge densities: en_0	
ρ	Charge density of the plasma, Sec. 3.1
ρ_b	Charge density of the beam, Sec. 3.1, Sec. 5.6.1, colormaps-full
Current densities: ecn_0	
\vec{j}	Total current density of plasma particles, Sec. 3.1
\vec{j}_b	Current density of the beam, Sec. 3.1
Charges: e	
q	Charge of a plasma macro-particle, Sec. 3.1
q_b	Charge of a beam particle, Sec. 3.3
Z	Charge of a plasma particle, Sec. 3.5
Currents: mc^3/e	
I_{b0}	Base beam current, Sec. 5.2, beam-current
I_b	Current of the beam slice, Sec. 6.1, xishape
Fields: $E_0 \equiv mc\omega_p/e$	
\vec{E}	Electric field in the plasma, Sec. 3.1
\vec{B}	Magnetic field in the plasma, Sec. 3.1
\vec{E}_r, \vec{B}_r	Auxiliary fields used in the kinetic plasma solver, Sec. 3.1
B_0	External longitudinal magnetic field, Sec. 3.1, Sec. 5.4, magnetic-field-type
B_{z0}	Variation amplitude for the external magnetic field, Sec. 5.4, magnetic-field
E_{az}	Average longitudinal electric field acting on the beam slice, Sec. 5.6.2, f(xi)
Potential: mc^2/e	
Φ	Wakefield potential, Sec. 3.2
a, a_0	Vector potential of a laser pulse, Sec. 3.5
Energies: mc^2	
W_{kin}	Kinetic energy of a plasma electron, Sec. 3.1
W_{ss}	Substepping energy for the beam, Sec. 5.2, beam-substepping-energy

Energy flux densities:		$n_0 mc^3$
\vec{S}	Total energy flux density, Sec. 3.4, Sec. 5.6.1, colormaps-full	
\vec{S}_f	Collective energy flux density, Sec. 3.4, Sec. 5.6.1, colormaps-full	
\vec{S}_e	Electromagnetic energy flux density, Sec. 3.4, Sec. 5.6.1, colormaps-full	
Energy fluxes:		$n_0 mc^5 / \omega_p^2$
Ψ	Total energy flux along the simulation window, Sec. 3.4, Sec. 5.6.2, f(xi)	
Ψ_w	Sum of Ψ and energy flux through window boundaries, Sec. 3.4, Sec. 5.6.2, f(xi)	
Ψ_f	Collective energy flux along the simulation window, Sec. 3.4, Sec. 5.6.2, f(xi)	
Ψ_e	Electromagnetic energy flux along the simulation window, Sec. 3.4, Sec. 5.6.2, f(xi)	
Energy densities:		$n_0 mc^2$
W	Total energy density, Sec. 3.4, Sec. 5.6.1, colormaps-full	
W_f	Collective energy density, Sec. 3.4, Sec. 5.6.1, colormaps-full	
Linear energy densities:		$n_0 mc^4 / \omega_p^2$
W_{int}	Linear density of the total energy, Sec. 3.4, Sec. 5.6.2, f(xi)	
dW_{int}	Difference between total and collective linear energy densities, Sec. 3.4, Sec. 5.6.2, f(xi)	
Distribution functions:		
f_{\perp}	Sec. 6.1, rshape	$\omega_p / (m^2 c^3)$
f_{4d}	Sec. 6.1, rshape	$\omega_p^2 / (m^2 c^4)$
f_{\parallel}	Sec. 6.1, eshape	$1 / (mc)$
Focusing strength:		$m\omega_p^2$
F_s	Strength of the external beam focusing, Sec. 5.2, loc-strength	
Dimensionless:		
q_i	Charge of i -th plasma macro-particle, Sec. 3.1	
A	Normalization factor for calculation of plasma currents and charge densities, Sec. 3.1	
\vec{e}_z	Unit vector in z -direction, Sec. 3.2	
N	Quantity used by the fluid solver instead of the electron density, Sec. 3.2	
γ	Relativistic factor of a plasma particle or of a fluid element, Sec. 3.2	
$G(\xi)$	Longitudinal profile of a laser pulse, Sec. 3.5	
P_f	Laser polarization factor, Sec. 3.5	
$\bar{\gamma}$	Average relativistic factor of a plasma particle in a laser field, Sec. 3.5	
N_r	Number of grid steps in the transverse direction, Sec. 5.1, r-step	
l	Number of twofold reductions of the time step for a low-energy beam particle, Sec. 5.2, beam-substepping-energy	
N_b	Number of beam macro-particles in the slice of current I_{b0} , Sec. 5.2.1, beam-particles-in-layer	
n_p, n_1, P	Plasma density multipliers: current value, amplitude, and additional parameter (sometimes) if the plasma density varies in z , Sec. 5.4.1, plasma-zshape	
D_{ss}	Maximum sub-stepping depth allowed for the kinetic plasma model (0...4), Sec. 5.4.1, substepping-depth	
A_{sub}	Sensitivity of the substepping trigger, Sec. 5.4.1, substepping-sensitivity	
d_b	Fraction of beam particles to output, Sec. 5.5, write-beam-particles	
η_{draw}	Fraction of the simulation window to be drawn as the full window, Sec. 5.6.1,	
N_{mr}	Number of grid points to be merged transversely into a single pixel on colored maps, Sec. 5.6.1, output-merging-r	
$N_{m\xi}$	Number of grid points to be merged longitudinally into a single pixel on colored maps, Sec. 5.6.1, output-merging-z	
X_m, Y_m	Substitutes for axis dimensions, Sec. 5.6.2, Sec. 5.6.3	
D_b	Fraction of beam macro-particles to be drawn, Sec. 5.6.3, draw-each	
h_{fig}	Height of various pictures in pixels, Sec. 5.6.3, beam-picture-height	
N_{bins}	Number of histogram bins, Sec. 5.6.4, histogram-bins	
γ_{min}	Minimum relativistic factor for the plasma particle to be drawn, Sec. 5.6.5, trajectories-min-energy	
C_{step}	Color step for visualization of particle energies, Sec. 5.6.5, trajectories-energy-step	
N_{col}	Ordinal number of a color in the palette, Sec. 5.6.5, trajectories-energy-step	
α_b	Angular spread of the beam slice, Sec. 6, angshape	
α_0	Maximum angular spread in the segment, Sec. 6, angspread	
I_a	Maximum current in the beam segment, Sec. 6.1, ampl	

Throughout the manual, the following highlighting conventions are used:

- (filename.ext) — names of various files (small typewriter font in parentheses);
- command -opt — execution commands (typewriter font);
- option — configuration option (boldface);

3 Underlying physics

3.1 Kinetic plasma model

The equations solved for the fields are Maxwell equations, which in the dimensionless variables take the form

$$\operatorname{rot} \vec{B} = \vec{j} + \vec{j}_b + \frac{\partial \vec{E}}{\partial t}, \quad \operatorname{rot} \vec{E} = -\frac{\partial \vec{B}}{\partial t}, \quad \operatorname{div} \vec{E} = \rho + \rho_b, \quad \operatorname{div} \vec{B} = 0. \quad (1)$$

Under the quasi-static assumption

$$\frac{\partial}{\partial z} = -\frac{\partial}{\partial t} = \frac{\partial}{\partial \xi}, \quad (2)$$

equations (1) result in

$$\frac{1}{r} \frac{\partial}{\partial r} r E_r = \rho + \rho_b - \frac{\partial E_z}{\partial \xi}, \quad \frac{1}{r} \frac{\partial}{\partial r} r B_r = -\frac{\partial B_z}{\partial \xi}, \quad (3)$$

$$\frac{1}{r} \frac{\partial}{\partial r} r (E_r - B_r) = \rho - j_z, \quad \frac{\partial E_z}{\partial r} = j_r, \quad \frac{\partial B_z}{\partial r} = -j_\varphi, \quad E_\varphi = -B_r. \quad (4)$$

Here we neglect the components j_{br} and $j_{b\varphi}$ of the beam current and put $j_{bz} = \rho_b$, since beam particles are assumed to move mostly in z -direction. To provide stability of the algorithm, we solve in finite differences, instead of (3), the following equations:

$$\frac{\partial}{\partial r} \frac{1}{r} \frac{\partial}{\partial r} r E_r - E_r = \frac{\partial(\rho + \rho_b)}{\partial r} - \frac{\partial j_r}{\partial \xi} - \tilde{E}_r, \quad \frac{\partial}{\partial r} \frac{1}{r} \frac{\partial}{\partial r} r B_r - B_r = \frac{\partial j_\varphi}{\partial \xi} - \tilde{B}_r, \quad (5)$$

where \tilde{E}_r and \tilde{B}_r are some predictions for fields E_r and B_r . These equations are obtained by differentiation of (3) and substitution of (4) into the result. Subtraction of the fields (with or without the tildes) from both sides of the equalities does not produce a big error if the predictions are close to final fields. The boundary conditions for equations (4)–(5) are those of a perfectly conducting tube of the radius r_{\max} :

$$E_r(0) = B_r(0) = B_\varphi(0) = E_z(r_{\max}) = B_r(r_{\max}) = 0, \quad \int_0^{r_{\max}} 2\pi r B_z dr = \pi r_{\max}^2 B_0, \quad (6)$$

where B_0 is an external longitudinal magnetic field, if any (the presence of this field does not change the axial symmetry of the system).

Each plasma macro-particle is characterized by 7 quantities: transverse coordinate (r), three components of the momentum (p_r , p_φ , and p_z), mass M , charge q , and ordinal number. Parameters of plasma macro-particles are initialized ahead of the beam (at $\xi = 0$) and then advanced slice-by-slice according to equations

$$\frac{d\vec{p}}{d\xi} = \frac{d\vec{p}}{dt} \frac{dt}{d\xi} = \frac{q}{v_z - 1} \left(\vec{E} + [\vec{v} \times \vec{B}] \right), \quad \frac{dr}{d\xi} = \frac{v_r}{v_z - 1}, \quad \vec{v} = \frac{\vec{p}}{\sqrt{M^2 + p^2}}. \quad (7)$$

If a particle hits the wall (at $r = r_{\max}$), it is returned to the simulation area to some near-wall location with zero momentum. Plasma current and charge density are obtained by summation over plasma macro-particles lying within a given radial interval:

$$\vec{j} = A \sum_i \frac{q_i \vec{v}_i}{1 - v_{z,i}}, \quad \rho = A \sum_i \frac{q_i}{1 - v_{z,i}}, \quad (8)$$

where A is a normalization factor. The denominator in (8) appears since the contribution of a “particle tube” to density and current depends on the macro-particle speed in the simulation window.

The plasma response is calculated layer-by-layer towards the decreasing ξ (from right to left in Fig. 2). As far as for calculation of fields we need ξ -derivatives of currents, the following predictor-corrector scheme is used. We first move plasma particles from layer a to layer b by the fields of the layer a , then calculate currents in layer b ,

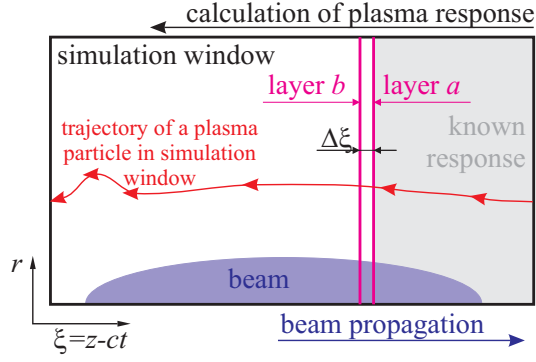


Figure 2: Calculation of plasma response in the quasi-static approximation.

then calculate all fields in layer b , then move plasma particles from layer a to layer b by average fields of layers a and b , then again calculate currents and fields in layer b , then again move plasma particles from layer a to layer b by the average fields. When the fields are calculated first time, the radial fields from the previous layer are taken as \tilde{E}_r and \tilde{B}_r . When the fields are calculated second time, the earlier found average radial fields are used as \tilde{E}_r and \tilde{B}_r . Also, special efforts are made to suppress a small-scale (of the grid step size) plasma density noise.

The algorithm allows easy shortening of the ξ -step in the regions of a fine field structure. The shortening is made automatically if the plasma current density $|j_z|$ exceeds some threshold value.

In the plane geometry, instead of equations (4), (5) we solve

$$\frac{\partial^2 E_x}{\partial x^2} - E_x = \frac{\partial(\rho + \rho_b)}{\partial x} - \frac{\partial j_x}{\partial \xi} - \tilde{E}_x, \quad \frac{\partial^2 B_x}{\partial x^2} - B_x = \frac{\partial j_y}{\partial \xi} - \tilde{B}_x, \quad (9)$$

$$\frac{\partial(E_x - B_y)}{\partial x} = \rho - j_z, \quad \frac{\partial E_z}{\partial x} = j_x, \quad \frac{\partial B_z}{\partial x} = -j_y, \quad E_y = -B_x, \quad \frac{\partial(E_x - B_y)}{\partial \xi} = j_x. \quad (10)$$

The last equation is used only at $x = 0.9 r_{\max}$ to find the integration constant for B_y . The boundary conditions in the plane case are

$$E_z(0) = B_x(0) = E_z(r_{\max}) = B_r(r_{\max}) = 0, \quad \int_0^{r_{\max}} B_z dx = r_{\max} B_0. \quad (11)$$

3.2 Fluid plasma model

In the fluid approximation, the plasma is characterized by the density n_e and momentum \vec{p} of the electron component. Plasma ions are the immobile background of the density $n_i = 1$. Motion of the electron fluid is governed by the equation

$$\frac{\partial \vec{p}}{\partial t} + (\vec{v} \nabla) \vec{p} = -\vec{E} - [\vec{v} \times \vec{B}], \quad (12)$$

which, together with (1) and

$$\vec{j} = -n_e \vec{v}, \quad \rho = 1 - n_e, \quad \vec{v} = \vec{p} / \gamma, \quad \gamma = \sqrt{1 + p^2}, \quad (13)$$

forms the complete set of equations. This set has two constants of motion. The first one was derived by Khudik and Lotov¹:

$$\vec{B} = \text{rot } \vec{p} + n_e B_0 (\vec{e}_z - \vec{v}), \quad (14)$$

where B_0 is the unperturbed longitudinal magnetic field ahead of the beam. The second one is well known and comes from conservation of the generalized momentum:

$$\Phi = \gamma - p_z, \quad (15)$$

where Φ is the wakefield potential:

$$E_z = -\frac{\partial \Phi}{\partial \xi}, \quad E_r - B_\varphi = -\frac{\partial \Phi}{\partial r}. \quad (16)$$

¹V.N.Khudik and K.V.Lotov, *Ion channels produced by ultrarelativistic electron beams in a magnetized plasma*. Plasma Physics Reports, v.25 (1999), N 2, p.149-159.

It is convenient to use the quantity $N = n_e(1 - v_z)$ instead of the electron density n_e and explicitly use the continuity equation which takes the form

$$\frac{\partial N}{\partial \xi} = \frac{1}{r} \frac{\partial}{\partial r} \frac{r N p_r}{\Phi}. \quad (17)$$

The final set of solved equations is, in the order of solving,

$$\frac{\partial \Phi}{\partial \xi} = -E_z, \quad \frac{\partial p_r}{\partial \xi} = \frac{\partial p_z}{\partial r} + B_\varphi + \frac{N p_\varphi B_0}{\Phi}, \quad N = 1 + \frac{1}{r} \frac{\partial}{\partial r} r \frac{\partial \Phi}{\partial r}, \quad (18)$$

$$\frac{\partial}{\partial r} \frac{1}{r} \frac{\partial}{\partial r} r p_\varphi - \frac{N p_\varphi}{\Phi} = -B_0 \frac{\partial N}{\partial r}, \quad p_z = \frac{1 + p_r^2 + p_\varphi^2 - \Phi^2}{2\Phi}, \quad \frac{\partial E_z}{\partial r} = -\frac{N p_r}{\Phi}, \quad (19)$$

$$B_r = -E_\varphi = -\frac{N p_r B_0}{\Phi} - \frac{\partial p_\varphi}{\partial \xi}, \quad B_z = \frac{1}{r} \frac{\partial}{\partial r} r p_\varphi + B_0 N, \quad (20)$$

$$\frac{\partial}{\partial r} \frac{1}{r} \frac{\partial}{\partial r} r B_\varphi - \frac{N}{\Phi} B_\varphi = \frac{\partial j_b}{\partial r} - p_z \frac{\partial}{\partial r} \frac{N}{\Phi} + \frac{p_r}{\Phi} \frac{\partial}{\partial r} \frac{r N p_r}{\Phi} + \frac{N p_r E_z}{\Phi^2} + \frac{N^2 p_\varphi B_0}{\Phi^2}. \quad (21)$$

Equations (18) are: the first equation of (16); the φ -component of (14) combined with (15); and the first equation of (4). Equations (19) are: the z -component of (14) differentiated with respect to r and combined with the third equation of (4); the definition of Φ (15) with the relativistic factor taken from (13); and the second equation of (4). Equations (20) are: the last equation of (4); the r -component of (14); and the z -component of (14). To obtain equation (21), we differentiate the z -component of the first equation in (1) with respect to r , use the expression (19) for $\partial E_z / \partial r$, and exclude ξ -derivatives of N , Φ , and p_r with the help of (17) and (18).

In equations (18)–(21), only two quantities (Φ and p_r) need to be advanced to the next layer in ξ , all the others can be expressed in terms of Φ and p_r within the layer. The initial conditions for (18)–(21) are $\Phi = 1$ and $p_r = 0$. The necessary boundary conditions are

$$p_\varphi(0) = p_\varphi(r_{\max}) = 0, \quad B_\varphi(0) = E_z(r_{\max}) = 0, \quad \left. \frac{\partial(r B_\varphi)}{\partial r} \right|_{r=r_{\max}} = 0. \quad (22)$$

Equations (18)–(21) are solved with the predictor-corrector scheme.

In the plane geometry, the solved equations are

$$\frac{\partial \Phi}{\partial \xi} = -E_z, \quad \frac{\partial p_x}{\partial \xi} = \frac{\partial p_z}{\partial x} + B_y + \frac{N p_y B_0}{\Phi}, \quad N = 1 + \frac{\partial^2 \Phi}{\partial x^2}, \quad \frac{\partial^2 p_y}{\partial x^2} - \frac{N p_y}{\Phi} = -B_0 \frac{\partial N}{\partial x}, \quad (23)$$

$$p_z = \frac{1 + p_x^2 + p_y^2 - \Phi^2}{2\Phi}, \quad \frac{\partial E_z}{\partial x} = -\frac{N p_x}{\Phi}, \quad B_x = -E_y = -\frac{N p_x B_0}{\Phi} - \frac{\partial p_y}{\partial \xi}, \quad B_z = \frac{\partial p_y}{\partial x} + B_0 N, \quad (24)$$

$$\frac{\partial^2 B_y}{\partial x^2} - \frac{N}{\Phi} B_y = \frac{\partial j_b}{\partial x} - p_z \frac{\partial}{\partial x} \frac{N}{\Phi} + \frac{p_x}{\Phi} \frac{\partial}{\partial x} \frac{N p_x}{\Phi} + \frac{N p_x E_z}{\Phi^2} + \frac{N^2 p_y B_0}{\Phi^2}, \quad (25)$$

$$p_y(0) = p_y(r_{\max}) = 0, \quad E_z(0) = E_z(r_{\max}) = 0, \quad \left. \frac{\partial B_y}{\partial x} \right|_{x=0} = \left. \frac{\partial B_y}{\partial x} \right|_{x=r_{\max}} = 0. \quad (26)$$

3.3 Beam model

The beam is modeled by macro-particles. Each beam macro-particle is characterized by its longitudinal position ξ_b , transverse position r_b or x_b , three components of momentum \vec{p}_b , charge q_b , and mass m_b . Equations of motion for the macro-particles are

$$\frac{dr_b}{dt} = v_{br}, \quad \frac{d\xi_b}{dt} = v_{bz} - 1, \quad \frac{d\vec{p}_b}{dt} = q_b \vec{E} + q_b [\vec{v}_b \times \vec{B}], \quad \vec{v}_b = \frac{\vec{p}_b}{\sqrt{m_b^2 + p_b^2}}. \quad (27)$$

These equations are solved with the modified Euler's method (midpoint method). The fields acting on the macro-particle are linearly interpolated to the predicted macro-particle location at the half time step. If a particle has a small longitudinal momentum and thus a high frequency of betatron oscillations, then the time step for this particle is automatically reduced.

With no external magnetic field ($B_0 = 0$), the angular momentum of beam particles must conserve, so the azimuthal component of the momentum $p_{b\varphi}$ is not changed according to (27), but reconstructed from the condition $r_b p_{b\varphi} = \text{const}$.

3.4 Energy fluxes and energy densities

In the presence of beams, there appears energy flows in the co-moving window². These flows are composed by the energy flow in the laboratory frame and the energy transfer due to motion of the window. We can write the perturbation to the dimensionless flux density of the electromagnetic energy

$$\vec{S}_e = -\vec{e}_z \frac{E^2 + B^2 - B_0^2}{2} + [\vec{E} \times \vec{B}], \quad (28)$$

and the total energy flux density in the co-moving window

$$\vec{S} = \vec{S}_e + \sum (\gamma - 1)(\vec{v} - \vec{e}_z), \quad (29)$$

where the summation is carried out over plasma particles in the unit volume. For the fluid plasma model, the energy flux density is

$$\vec{S}_f = \vec{S}_e + n_e(\gamma - 1)(\vec{v} - \vec{e}_z). \quad (30)$$

The difference of the two, $\vec{S} - \vec{S}_f$, is the measure of the energy carried in the form of a thermal motion of plasma particles.

Integrating (28)–(30) across the simulation window gives us the energy fluxes against the z -axis:

$$\Psi_e = - \int_0^{r_{\max}} S_{ez} 2\pi r dr, \quad \Psi = - \int_0^{r_{\max}} S_z 2\pi r dr, \quad \Psi_f = - \int_0^{r_{\max}} S_{fz} 2\pi r dr. \quad (31)$$

The drive beam puts energy to some point of the simulation window, and then this energy flows backward or transversely until it exits the window or gets taken by a witness beam. The energy loss through transverse boundaries is taken into account by the quantity

$$\Psi_w = \Psi + \int_{\xi}^0 2\pi r_{\max} S_r(r_{\max}, \xi') d\xi', \quad (32)$$

which is the measure of beam-plasma energy exchange:

$$\frac{\partial \Psi_w}{\partial \xi} = \int_0^{r_{\max}} j_{bz} E_z 2\pi r dr. \quad (33)$$

The derivative $\partial \Psi_w / \partial \xi$ must be zero in the absence of beams; this can be used as a good test of precision for simulations. The difference between Ψ and Ψ_f can serve as a measure of the lost energy which cannot be retrieved by the accelerated beam. Formulae (31)–(33) are for the axisymmetric case, their modification for the plane geometry is straightforward.

The total energy density and fluid energy density are defined in the straightforward way:

$$W = \frac{E^2 + B^2 - B_0^2}{2} + \sum (\gamma - 1), \quad W_f = \frac{E^2 + B^2 - B_0^2}{2} + n_e(\gamma - 1), \quad (34)$$

correspondingly; summation is over plasma particles the unit volume.

3.5 Laser beams

The shape of the laser pulse is characterized by the envelope $a(r, \xi)$ of the dimensionless vector potential. There are two regimes of laser evolution. In the regime of unperturbed propagation, the pulse shape is

$$a^2 = \frac{a_0^2 \sigma_{rl0}^2}{\sigma_{rl}^2} e^{-r^2 / \sigma_{rl}^2} G(\xi), \quad (35)$$

where the beam radius σ_{rl} depends on the propagation time t :

$$\sigma_{rl} = \sigma_{rl0} \sqrt{1 + t^2 / Z_R^2}, \quad Z_R = \sigma_{rl0}^2 \omega_0 \quad (36)$$

²K.V.Lotov, *Blowout regimes of plasma wakefield acceleration*. Phys. Rev. E, v.69 (2004), N 4, p.046405.

(Z_R is the Rayleigh length, ω_0 is the laser frequency), and $G(\xi)$ is the longitudinal profile of the pulse:

$$\text{Cosine-like:} \quad G(\xi) = \frac{1}{2} \left[1 + \cos \left(\frac{2\pi(\xi - \xi_c)}{L_l} \right) \right], \quad L_l = 2\sigma_{z_l}\sqrt{\pi}, \quad |\xi - \xi_c| < L_l/2; \quad (37)$$

$$\text{Gaussian:} \quad G(\xi) = \exp \left(-\frac{(\xi - \xi_c)^2}{\sigma_{z_l}^2} \right), \quad |\xi - \xi_c| < 5\sigma_{z_l}. \quad (38)$$

The center of the laser pulse moves backwards in the co-moving frame:

$$\xi_c = \xi_{t_0} - \left(1 - \sqrt{1 - \omega_0^{-2}} \right) t. \quad (39)$$

There could be up to 5 laser pulses in the simulation window.

In the regime of self-consistent evolution, the initially generated laser pulse has the shape

$$a^2 = a_0^2 e^{-r^2/\sigma_{r_{i0}}^2} G(\xi) \quad \text{or} \quad a^2 = a_0^2 e^{-(x-x_l)^2/\sigma_{r_{i0}}^2} G(\xi) \quad (40)$$

in cylindrical and plane geometries, respectively. Alternatively, a pulse of any shape can be generated with an external script. The pulse evolves according to envelope equations from Mora&Antonsen [Phys. Plasmas **4**, 217 (1997)].

The laser pulse acts on plasma particles with the ponderomotive force

$$\vec{F} = -\frac{P_f Z^2}{2\bar{\gamma} M_p} \nabla a^2, \quad \bar{\gamma} = \sqrt{\gamma^2 + \frac{Z^2 a^2}{M_p^2}}, \quad (41)$$

where P_f is the factor accounting for pulse polarization, Z is the particle charge in units of the elementary charge e , M_p is the particle mass in units of the electron mass m , γ is the relativistic factor of particle. There is no force acting on beam particles. This force cannot be consistently simulated since the expression (41) is not valid if the particle velocity is close to the group velocity of the laser pulse. Therefore, the model is correct only if the particle beam and the laser pulse do not overlap, or this overlapping is inessential.

The laser pulse cannot work simultaneously with the fluid plasma model.

4 Running the code

4.1 Overview

To run LCODE, execute the file (`lcode.exe`) (Windows) or (`lcode`) (UNIX-like, execute with `./lcode`) in the folder where the input files are located (Sec. 4.2). If needed, provide configuration file(s) and/or options to LCODE, as described in Sec. 4.3. LCODE will start creating the output files with simulation results in the current directory. You may control the execution interactively, as described in Sec. 4.4. Upon completing the simulations, LCODE process will exit, for the explanation of the exit codes refer to Sec. 4.5. Using the MPI-enabled parallel version of LCODE is detailed in Sec. 4.6.

4.2 Input files

Possible (optional) input files are:

(`lcode.cfg`): the default configuration file (Sec. 5);

(`beamfile.bin`): the beam state file (Sec. 7.1);

(`beamfile.bit`): the continuation run indicator (Sec. 7.2);

(`plasma.bin`): the default plasma state file (Sec. 7.3);

(`fields.bin`): the default fields state file (Sec. 7.4);

arbitrarily named: other configuration files (Sec. 6), the beam constructor file (see **beam-profile**), initial states of plasma and fields (Sec. 5.4.1).

4.3 Configuration options and files

Additional command-line options can be provided after the executable name:

- Options `--option=value` overwrite options used in the main configuration file `lcode.cfg`.
- Directives `filename.ext` include other files containing configuration options.
- Special options interrupt the normal process of parsing command-line parameters and terminate execution of the program with the following actions:
 - `--help` or `--usage` outputs a brief description of all possible configuration options.
 - `--dump` or `--dump-config` outputs the already read values of configuration options to console. To save the output to a file (`config.cfg`), execute `lcode.exe --dump-config > config.cfg` (Windows) or `./lcode --dump-config > config.cfg` (UNIX-like).
 - `--dump-defconfig` outputs the the configuration file with default values of options to console. To save it to a file (`default.cfg`), execute `lcode.exe --dump-defconfig > default.cfg` (Windows) or `./lcode --dump-defconfig > default.cfg` (UNIX-like).
 - `--dump-docconfig` outputs the the configuration file with default values of options, but in a more detailed format. To save it to a file (`docconfig.cfg`), execute `lcode.exe --dump-docconfig > docconfig.cfg` (Windows) or `./lcode --dump-docconfig > docconfig.cfg` (UNIX-like).
 - `--beamfile-compose` allows concatenating and sorting files in beamfile.bin format (section 7.1). Please refer to the section 8.1 for details.
 - `--beamfile-inspect` allows inspecting the contents of the files in beamfile.bin format (section 7.1). Please refer to the section 8.2 for details.

If an option occurs several times in configuration files or command line, then the later value is used. The order of reading the values is the following:

1. Initially all options are set with default hard-coded values (the ones specified as default in this manual, Sec. 5).
2. The main configuration file 'lcode.cfg', if present, with all the files included. The file is read from the beginning to the end, with the included files, if any.
3. The command-line options processed left-to-right, if provided, with the included files, if any.

Here are some examples of using command-line options:

```
./lcode
Executes LCODE with the values read from lcode.cfg, if present. (UNIX-like)
```

```
lcode.exe filename.cfg --beam-tune-charge=y
The same as above, but also reads values from (filename.cfg) and explicitly defines the beam-tune-charge option. (Windows)
```

```
lcode.exe filename1.cfg filename2.cfg --dump
First reads values from (lcode.cfg), if available; then reads values from (filename1.cfg) and (filename2.cfg); then prints the resulting set of values to the screen. Simulations are not started. (Windows)
```

```
./lcode filename1.cfg .cfg --time-limit=1000 --dump > new.cfg
First reads values from (lcode.cfg), if available; then reads values from (filename1.cfg); modifies the value of th option time-limit; then writes the updated version of the config file to (new.cfg). Simulations are not started. (UNIX-like)
```

```
./lcode --dump-defconfig > lcode.cfg
Creates a default configuration file (lcode.cfg). Simulations are not started. (UNIX-like)
```

The option values are validated after reading. If some values are invalid, then the program attempts an automatic 'config recovery' which consists of resetting the invalid values to the hardcoded defaults. This action is indicated by warning messages. An example of a config recovery session is:

```
invalid histogram-bins=0 (Must be positive and <= 300) was reset to default 300
config recovered
```

```
Error filling config:  invalid config, some defaults used
The config is still valid though
Trying to use a recovered config
```

If the recovery has been completed successfully, the program attempts execution with the recovered config.

The final (possibly recovered) configuration values at the start of computations are written to (`lcode.runas.cfg`) to ease the diagnostics (see **save-config**, **save-config-filename**).

4.4 Interactive control

If the program is running in the terminal mode, its execution can be controlled by pressing some keys at the terminal:

- ' ,' (comma): pause the execution before the next time step, can be used repeatedly to pause after each time step;
- ' .' (dot): stop the execution after finishing the time step, the run can be resumed afterwards;
- ' ' (space): pause the execution immediately;
- 'esc' (escape): terminate the execution immediately;
- '*' (any key): resume the paused execution.

Note that the interactive control features are not tested in combination with parallel computations.

4.5 Exit codes

The exit codes are:

- 0 — execution ends successfully;
- 1 — execution fails, the program prints an error message and terminates;
- 2 — the program was stopped manually with the dot key;
- 3 — the program was interrupted manually with the escape key.

4.6 Parallel calculations with the MPI-enabled version

LCODE may be compiled with the ability of computing several time steps simultaneously by several processes executing in parallel. MPI (Message Passing Interface) is used for interprocess communication. In this mode the first process reads the beam file from disk and directs the new beam generation data to the input of the process 'trailing' it. The following processes also form a data processing chain, with the outputs of the former ones connected to the inputs of the latter ones. The last process writes the data to disk again.

Note that MPI-enabled version does not keep the whole beam in RAM and is considerably less RAM-hungry than the regular version. Also keeping the beam on disk removes the limitation on the amount of particles in the beam (see option **max-ram-megabytes** for details).

This way several cores of a single processors, multiple processors of a single system or even multiple processors of a distributed system with a shared storage could be used to speed up LCODE simulations by calculating more than one time step in a single pass.

For the instructions on running the MPI-enabled version please contact your system administrator. Note that the MPI-enabled version must be compiled separately for different MPI execution environments. If you want to request a specific MPI-enabled build for your configuration, please specify your operating system version, MPI implementation vendor and version. If you are specifically designing your computer system to run LCODE, please consider using the latest stable Debian GNU/Linux system with OpenMPI, as this is the most tested platform by now.

5 Configuration file

The configuration file is a text file containing the list of options in the form

```
option=value  or  option = value.
```

The order of options is of no importance. If an option is specified several times, the later value is used. Several options may coexist on the same line of the file, if they are separated by semicolons. Semicolons may be omitted in several cases, but it is strongly recommended not to rely on that. The configuration file can contain comments or empty lines which are ignored by the program, but improve visual readability of the file.

Comments begin with # and extend to the end of line.

In this section, configuration options are described like this:

option, *type* (default value): brief description
Detailed description, if necessary.

Possible types of options are:

choice: a value from a predefined set.

float: a floating-point number, may be in scientific notation.

string: a string (multiple characters). Strings with spaces, semicolons or hash signs must be enclosed in double quotes, multiline strings must be enclosed in triple double quotes.

multichoice: multiple values from the predefined set, separated with commas.

y/n: ‘yes’ or ‘no’. Brief forms ‘y’ and ‘n’ are also possible.

The following is the list of options grouped by purpose. The options present in (`lcode.runas.cfg`), but not described here, are under development.

5.1 Simulation area

geometry, *choice* (c): The geometry of the problem:

‘c’ or ‘axisymmetric’: Axisymmetric (cylindrical) geometry

‘p’ or ‘plane’: Plane (2d Cartesian) geometry

window-width, *float* (5): Transverse size of the simulation window, r_{\max}

The radius in the cylindrical geometry or the full width in the plane geometry.

r-step, *float* (0.05): Transverse grid step, Δr

The number of grid steps in the transverse direction, N_r , must not be too large: $N_r = r_{\max}/\Delta r \leq 40000$.

Otherwise Δr is automatically increased.

window-length, *float* (15): Length of the simulation window, ξ_{\max}

xi-step, *float* (0.05): Longitudinal grid step, $\Delta \xi$

time-limit, *float* (200.5): Time limit for the run, t_{\max}

Rounds to the nearest multiple of **time-step**. A special case of zero **time-limit** and **time-step** is allowed, in this mode LCODE generates the initial beam file and exits.

time-step, *float* (25): Main time step for the beam, Δt

continuation, *choice* (n): Mode of plasma continuation (Fig. 3):

‘n’ or ‘no’: Evolution of the beam. At each time step, the beam enters an unperturbed plasma with a given density profile.

‘y’ or ‘beam’: Evolution of the beam sequence. At each time step (except the first) the beam enters the perturbed plasma; the plasma state is taken from the end of the previous simulation window. Does not work for the fluid plasma model.

‘Y’ or ‘longplasma’: Evolution of the plasma. A long beam creates the wake, and long-term behavior of this wake is followed by the sequence of simulation windows. In this mode, only a rigid beam can extend to several simulation windows. Does not work for the fluid plasma model.

Latter two regimes need $\Delta t = \xi_{\max}$, otherwise Δt is automatically corrected.

5.2 Particle beams

beam-current, *float* (0.1): Base beam current (in 17 kA), I_{b0}

The common multiplier (in units of $mc^3/e \approx 17\text{kA}$) for dimensionless beam currents specified in **beam-profile**. In the plane geometry corresponds to the current through c/ω_p in the third dimension. Also the unit current for beam macro-particles.

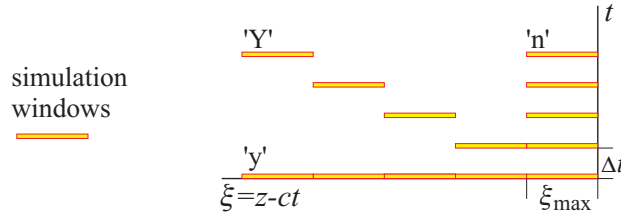


Figure 3: Illustration of continuation modes.

rigid-beam, *y/n* (n): Switch for evolution of the beam

‘y’ or ‘yes’: A rigid (not evolving in time) distribution of the beam current.

‘n’ or ‘no’: The beam is modeled by macro-particles.

beam-substepping-energy, *float* (2): Substepping energy for the beam, W_{ss}

The threshold of reducing the time step for beam particles. For each beam particle, the minimal integer l is found that meets the condition $2^{2l} \sqrt{m_b^2 + p_{bz}^2} > W_{ss}$, and the reduced time step $\Delta t' = \Delta t / 2^l$ is then determined. Plasma fields are calculated with periodicity Δt , and each beam particle is propagating in these fields with its own time step $\Delta t'$. This feature is particularly useful if low energy beam particles are present in the system, which otherwise would require undesirable reduction of the main time step Δt .

focusing, *choice* (n): External focusing for the beam:

‘n’ or ‘no’: No focusing

‘c’ or ‘cosine’: Cosine-varying focusing force. Each beam particle (located at radius r_b) at each time step gets the extra radial momentum $\Delta p_{\text{foc}} = F_s r_b \Delta t \cos(2\pi t / t_F)$.

‘r’ or ‘rectangular’: Piecewise-constant focusing force. Each beam particle (located at radius r_b) at each time step gets the extra radial momentum $\Delta p_{\text{foc}} = \pm F_s r_b \Delta t$, where “+” is chosen if the fractional part of $(t/t_F + 0.25)$ is less than 0.5, and “-” is chosen otherwise.

In the plane geometry, Δp_{foc} is the addition to x -momentum, and the distance between the particle and the midplane of the simulation window is used instead of r_b .

foc-period, *float* (100): Period of the external focusing, t_F

foc-strength, *float* (0.01): Strength of the external focusing, F_s

5.2.1 Newly generated beams

The following beam options determine parameters of newly generated particle beams or rigid beams. If the beam is allowed to evolve by **rigid-beam** and the files (`beamfile.bit`) and (`beamfile.bin`) are present in the working folder, then the beam state is imported from (`beamfile.bin`), the time is read from (`beamfile.bit`), and the following options are ignored.

beam-particles-in-layer, *integer* (200): Number of beam particles in the layer (≤ 100000), N_b

A beam slice which has the current I_{b0} and length $\Delta \xi$ contains N_b macro-particles. Beam slices with lower currents have correspondingly fewer macro-particles.

beam-profile, *string* (“xishape=cos, length=1”): Initial distribution of beam particles

The name of the file that specifies the initial distribution of beam particles in 6d phase space, or the initial beam distribution itself (as a multiline description enclosed in triple quotes). If the value consists of a single line without spaces or equal signs, it is interpreted as a filename to read the beam distribution from; otherwise the value itself is considered the beam distribution description. The format of beam distribution is described in Sec. 6.

beam-tune-charge, *y/n* (n): Tuning the charge of beam particles to match the beam profile better

‘n’ or ‘no’: All beam particles are equally charged. Only the absolute value of the charge can be different. Consequently, the beam current can have only discrete values and therefore slightly differs from the specified value.

‘y’ or ‘yes’: The charge of particles in each beam slice is slightly modified to better match the specified beam profile. This option lowers the shot noise produced by the beam.

rng-seed, *integer* (1): Random generator seed

An integer number initiating the generator of random numbers. Different seeds generate different statistical ensembles for the beam.

5.3 Laser beams

LCODE currently supports either of the two laser beam models: unperturbed propagation or self-consistent evolution (Sec. 3.5).

laser, *y/n* (n): Switch for laser beams:

‘n’ or ‘no’: No laser beam in the simulation window.

‘y’ or ‘yes’: A laser beam is present.

laser-evolution, *y/n* (y): Self-consistent description of laser beam evolution:

‘n’ or ‘no’: The model of unperturbed propagation is used, as if the pulse(s) propagate(s) in a uniform unperturbed plasma of unit density (Sec. 3.5).

‘y’ or ‘yes’: Self-consistent description of laser beam evolution.

The last option is ignored if **laser** = **n**.

5.3.1 Self-consistent evolution of the laser beam

States of the laser beam are saved in files named (**1s?????.??? .swp**), where (?????.???) is time. Exchange of laser information between consecutive time slices is through these files, so simulations of laser evolution currently require much writing to and reading from disk. It is recommended to run laser simulations from a virtual disk located in operative memory rather than from a hard disc.

The following options are applicable only if **laser-evolution** = **y**.

laser-amplitude, *float* (0.5): Initial amplitude of the laser pulse, a_0

laser-xi-sigma, *float* (2): Initial length of the laser pulse, σ_{z_l}

laser-xi-center, *float* (-5): Initial location of the laser pulse, ξ_c

The ξ -position of the laser pulse center in the simulation window. Must be inside the window by at least **laser-xi-sigma**, i. e. not closer than **laser-xi-sigma** to both the front and the back of the window.

laser-r-autocenter, *y/n* (n): Automatic centering the laser pulse in transverse direction

If ‘y’, ignores the value of **laser-r-center** and automatically position the pulse on the axis (at the middle of the window in plane geometry).

laser-r-center, *float* (0): Transverse position of the laser pulse, x_l

Used in the plane geometry only. Must be inside the window by at least **laser-r-sigma**, i. e. not closer than **laser-r-sigma** to the sides of the window. May be overridden with **laser-r-autocenter**.

laser-r-sigma, *float* (1): The initial width of the laser pulse, σ_{r_l0}

laser-wavenumber, *float* (250): Laser wavenumber, k_0

Also the laser frequency $\omega_0 = k_0$.

laser-polarization, *float* (0.5): Polarization factor, P_f

A multiplier that reflects the dependence of the ponderomotive force on laser polarization.

laser-steps-in-dt, *integer* (1): Laser substepping divisor, N_{laser}

Makes the time step for laser evolution equal $\Delta t/N_{laser}$.

laser-shape, *choice* (g): Longitudinal profile of the laser pulse, $G(\xi)$:

‘g’ or ‘gauss’: Gaussian, Eq. (38),

‘c’ or ‘cosine’: cosine, Eq. (37).

5.4 Plasma

plasma-model, *choice* (P): Plasma model:

‘f’ or ‘fluid’: The fluid model, Sec. 3.2. It is the fastest one, but works only for the initially uniform plasma with immobile ions. Neither wave-breaking, nor near-wall plasma perturbations are allowed.

‘P’ or ‘newparticles’: New kinetic model described in Sec. 3.1.

magnetic-field, *float* (0): Variation amplitude for the external longitudinal magnetic field, B_{z0}

For zero B_{z0} , the code runs faster since some equations (which are identically zeros) are not solved.

magnetic-field-type, *choice* (c): Time dependence of the external magnetic field seen by the beam:

‘c’ or ‘constant’: Always $B_0 = B_{z0}$.

‘r’ or ‘random’: B_0 is a random value between 0 and B_{z0} for each time step.

‘p’ or ‘periodic’: $B_0 = B_{z0} \cos(2\pi t/t_B)$.

magnetic-field-period, *float* (200): Period of magnetic field oscillations, t_B

Used only with the periodic external magnetic field.

5.4.1 Options specific to particle plasma models

These options have effect only if **plasma-model** is a kinetic one.

plasma-particles-per-cell, *int* (10): Number of plasma macro-particles per transverse grid cell

This option determines the number of macro-particles per transverse grid cell for plasma electrons (the total number of particles must be ≤ 100000). If mobile ions are enabled (**ion-model** = ‘Y’), the same number of macro-particles is added to cell for plasma ions. Particles are added only to cells where the plasma density according to **plasma-profile** is greater than zero.

plasma-particles-number, *int* (1000): Total number of plasma macro-particles for electrons (≤ 100000)

OBSOLETE. All plasma electrons are modeled by this number of macro-particles. Mobile ions, if chosen, are modeled by the same number of heavier macro-particles. When this option is used **plasma-particles-per-cell** is not taken into account. This option should not be used and one should transition to **plasma-particles-per-cell** instead.

plasma-profile, *choice* (1): The initial transverse profile of the plasma density (Fig. 4):

‘1’ or ‘uniform’: Uniform (= 1) up to the walls.

‘2’ or ‘stepwise’: Uniform (= 1) up to r_p , zero at $r > r_p$.

‘3’ or ‘gaussian’: Gaussian $n(r) = \exp(-r^2/2r_p^2)$, zero at $r > 5r_p$; obtained by variation of macro-particles weights.

‘4’ or ‘arbitrary’: Arbitrary, with particle parameters imported from plasma-input-file and initial fields from fields-input-file.

‘5’ or ‘channel’: Zero up to r_p , uniform (= 1) at $r > r_p$.

‘6’ or ‘sub-channel’: Constant (n_{p2}) up to r_{p2} , then linear growth from n_{p2} to 1 between r_{p2} and r_p , then 1 at $r > r_p$; obtained by variation of macro-particles weights.

For the plane geometry, the distance to the midplane $|x - r_{\max}/2|$ is used instead of r .

plasma-width, *float* (2): Main parameter of initial plasma density distributions, r_p

plasma-width-2, *float* (1): Auxiliary parameter of initial plasma density distributions, r_{p2}

plasma-density-2, *float* (0.5): Auxiliary parameter of initial plasma density distributions, n_{p2}

plasma-input-filename, *string* (“plasma.bin”): Filename for importing plasma particles state.

fields-input-filename, *string* (“fields.bin”): Filename for importing initial fields state.

path-to-plasma-state, *string* (“.”): Relative or absolute path to plasma state files

These options allow to specify the initial plasma state (at $\xi = 0$) dependant on propagation distance (t). The filenames must be in the form (fname****.bin), where (fname) are specified by these options and (****) is time (or equivalently the propagation distance) in the 5-digit representation (Sec. 5.6.2). If there is no exact match for the current time step, the plasma state with the closest time is taken. In the case of the default values (“plasma.bin” and “fields.bin”), these files are used for all time steps. This options are ignored in case of **continuation** = y/Y.

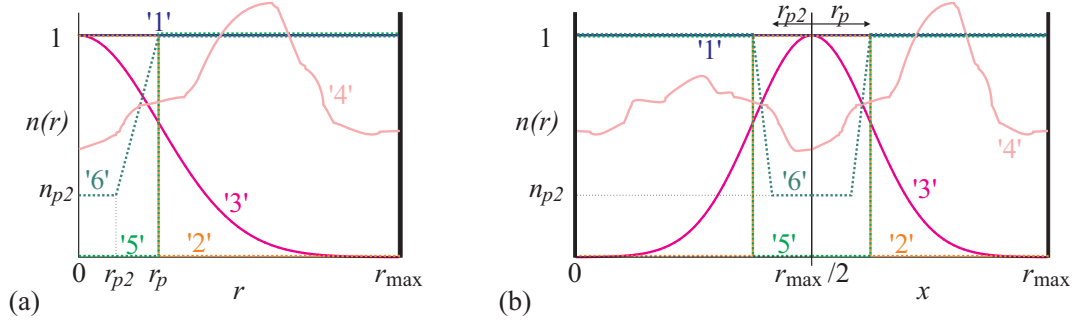


Figure 4: Illustration of possible plasma profiles in axisymmetric (a) and plane (b) geometries.

plasma-zshape, *string* (""): Longitudinal plasma density profile

This option defines a longitudinal plasma density profile, i.e. the plasma density $n_p(z)$. In the case of radially non-uniform plasmas, $n_p(z)$ is multiplied by the radial density profile $n(r)$ defined by **plasma-profile**. The longitudinal profile is specified in consecutive segments, one segment per line. Each line consists of a segment length l_p (float), a characteristic density value n_1 (float), a letter defining the segment shape (char) and an additional parameter P (float) used for some shapes.

The available segment shapes are:

'c' or 'c': Shifted cosine,	$n_p(l_m) = 0.5 n_1 (1 - \cos(2\pi l_m / l_p))$
't' or 't': OBSOLETE. Linear rise from 0 to n_1 ,	$n_p(l_m) = n_1 l_m / l_p$
'T' or 'T': OBSOLETE. Linear decrease from n_1 to 0,	$n_p(l_m) = n_1 (1 - l_m / l_p)$
'l' or 'l': OBSOLETE. Constant,	$n_p(l_m) = n_1$
'L' or 'L': Linear rise/decrease from n_1 to P ,	$n_p(l_m) = n_1 (1 - l_m / l_p) + P l_m / l_p$
'h' or 'half-cos': Rising half-period of the shifted cosine,	$n_p(l_m) = 0.5 n_1 (1 - \cos(\pi l_m / l_p))$
'b' or 'b': Decreasing half-period of the shifted cosine,	$n_p(l_m) = 0.5 n_1 (1 + \cos(\pi l_m / l_p))$
'g' or 'g': Decreasing part of Gaussian function with $\sigma = l/6$,	$n_p(l_m) = 0.5 n_1 \exp(-18 l_m^2 / l_p^2)$
'G' or 'G': Parameterized curve, rising from 0 to n_1 ($l_m \rightarrow \infty$),	$n_p(l_m) = n_1 (1 - \exp(-l_m / P))$
'e' or 'e': Parameterized curve, rising exponentially from n_1 ,	$n_p(l_m) = n_1 \exp(l_m / P)$
'E' or 'E': Parameterized curve, rising from $n_1/2$ to n_1 ($l_m \rightarrow \infty$),	$n_p(l_m) = n_1 (1 - 0.5 \exp(-l_m / P))$

At each time step, the plasma density is calculated as the value of the corresponding function in the middle of the time step (at $l_m = t - \Delta t/2 - l_{p0}$, where the segment begins at $z = l_{p0}$). If the total length of the segments is too short, then $n_p = 1$ in the uncertainty region. If the calculated plasma density is below 10^{-5} , then $n_p = 10^{-5}$ is set.

Example: `plasma-zshape = ""`

```
100 0 L 1.5
200 1.5 L 1.5
1500 3 E 150
""
```

Here the density n_p rises linearly from 0 to 1.5 for the first 100 units of time ($t \in [0; 100]$), stays at 1.5 for the next 200 units ($t \in [100; 300]$), and rises from 1.5 to approx. 3 as $n_p = 3 - 1.5 \exp(-(t - 300)/150)$ for the next 1500 units ($t \in [300; 1800]$). It defaults to 1 in the undefined region at $t > 1800$.

If this option is successfully enabled, LCODE outputs the length ($t - \Delta t/2$) at which the density is calculated and the plasma density n_p to (`plzshape.dat`), new line added each time step. It is recommended to check that this file is created and actually contains the desired plasma profile to make sure that the option is used correctly.

plasma-temperature, *float* (0): Initial temperature of mobile plasma particles in units of mc^2

ion-model, *choice* (y): Model of plasma ions:

- 'Y' or 'mobile': Half of plasma macro-particles are single-charged mobile ions initially located at the same positions as plasma electrons.
- 'y' or 'background': Ions are immobile background charge. If **plasma-profile** = '4', then the background ion density is the same as for uniform plasma.
- 'n' or 'absent': No ions, plasma electrons are initially at rest.

ion-mass, *float* (1836): Ion mass in units of the electron mass (for mobile ions)

substepping-depth, *integer* (3): Maximum sub-stepping depth allowed (0...4), D_{ss}

Substepping is usually needed for strongly nonlinear wakefields when some plasma particles are close to trapping. If necessary, the longitudinal grid step can be automatically reduced up to $10^{D_{ss}}$ times with respect to the basic **xi-step**.

substepping-sensitivity, *float* (0.2): Sensitivity of substepping trigger, A_{sub} .

If the longitudinal current density (j_z) is so high that the product of $|j_z|$ and ξ -step exceeds A_{sub} at some point, then the ξ -step is automatically divided by 10 (if allowed by **substepping-depth**). Reverse action (increasing the ξ -step) is taken when j_z gets small again.

trapped-path-limit, *float* (0): Path limit for trapped plasma particles, L_{trap}

With this option, it is possible to treat trapping of plasma particles by the wakefield (to the extent allowed by the quasi-static approximation). The charge of a macro-particle is put to zero when the time spent by this macro-particle in the simulation window exceeds L_{trap} . With this trick we obtain the correct plasma state and fields at the distance L_{trap} from the beam entrance to the plasma even if some plasma particles get trapped by the wakefield. It is necessary to put $L_{trap} \gg \xi_{max}$, otherwise the result will have no physical meaning. Zero value of L_{trap} switches this option off.

For every “trapped” macro-particle, 10 values are appended to file (**captured.pls**) (one particle per line):

1. Time
2. Number of the macro-particle (which contains information on its initial position)
3. Final ξ -coordinate
4. Final transverse coordinate
- 5-7. Final r -, φ -, and z -components of the particle momentum
8. Mass of the macro-particle
9. Charge-to-mass ratio
10. Relativistic factor

5.4.2 Option specific to the fluid plasma model

viscosity, *float* (0): Artificial viscosity

Artificial viscosity is used for suppressing high-frequency numerical noises or forcing the fluid model to work beyond the applicability area. Reasonable values are between 0 and 0.01.

5.5 Every-time-step diagnostics

If activated, these diagnostics work at each main time step Δt .

indication-line-format, *choice* (1): Format of the on-screen progress indication:

‘1’ or ‘eachdt’: One line each time step: time, total number of survived beam macro-particles, maximum and minimum electric field E_z on the axis.

‘2’ or ‘eachdxi’: One line each ξ -step: time, $|\xi|$, E_z on axis, total energy flux Ψ , number of beam macro-particles in this layer, number of sub-steps in ξ within the last ξ -step.

Location of the axis is determined by **axis-radius**. After finishing a time step (just before drawing pictures), the word “finished” is printed.

output-Ez-minmax, *y/n* (n): Write absolute extrema of the on-axis E_z into **(emaxf.dat)**

output-Phi-minmax, *y/n* (n): Write absolute extrema of the on-axis Φ into **(gmaxf.dat)**

output-Ez-local, *y/n* (n): Write local extrema of the on-axis E_z into **(elocf.dat)**

output-Phi-local, *y/n* (n): Write local extrema of the on-axis Φ into **(glocf.dat)**

If enabled, a line of 5 values is appended to the corresponding file immediately after an extremum is found:

1. Current time t
2. The maximum value of the quantity
3. ξ -coordinate of this maximum
4. The minimum value of the quantity (earlier found in case of local extrema)
5. ξ -coordinate of this minimum

Locations of the potential extrema are calculated more precisely than those of the field extrema. The latter are found as multiples of the grid step $\Delta\xi$.

write-beam-particles, y/n (n): Output of individual characteristics of beam particles

If the diagnostics is enabled, then the following information about selected beam particles is appended to file (`partic.swp`) at every time step, one line (9 values) per particle:

1. Time t ,
2. Longitudinal coordinate ξ_b ,
3. Transverse coordinate r_b or x_b ,
4. Longitudinal momentum p_{bz} ,
5. Transverse momentum p_{br} or p_{bx} ,
6. Angular momentum M_b or third component of the momentum p_{by} ,
7. Charge-to-mass ratio (absolute value),
8. Current carried by the particle,
9. Ordinal number.

The same particle characteristics can be also extracted from (`beamfile.bin`).

write-beam-particles-each, *integer* (1000): Fraction of beam particles to output, d_b

A beam particle is selected for output if its ordinal number is a multiple of d_b .

write-beam-particles-from, *float* (0): Right limit.

write-beam-particles-to, *float* (-10): Left limit

Only beam particles located between these two non-positive values are selected for output.

write-beam-particles-q-m-from, *float* (0): Lower limit for filtering beam particles by their q/m ratio

write-beam-particles-q-m-to, *float* (0): Upper limit for filtering beam particles by their q/m ratio

The interval of charge-to-mass ratios in which particles are written to (`partic.swp`). Equal values of these parameters disable filtering.

output-lost-particles, y/n (n): Output of lost particles to (`beamlost.dat`)

If enabled, then beam particles which exit the simulation window are kept in file (`beamlost.dat`). One line of 9 values is written for each particle. These values correspond to the last time particle was in the simulation window. The file format is the same as for (`partic.swp`).

5.6 Periodical diagnostics

These diagnostics are periodically triggered with the time interval given by

output-time-period, *float* (100): Time periodicity of detailed output, Δt_{out}

If $\Delta t_{\text{out}} < \Delta t$, then each time step is diagnosed. The first time step is always diagnosed.

5.6.1 Colored maps

These keys control output of various quantities as functions of r and ξ , either in the form of a colored map, or in the form of a data array.

The colored maps are produced as separate files named (`??*****[w].png`) where (??) stands for two-character quantity abbreviation, (*****) is the time of output, and the optional suffix 'w' denotes subwindow output.

Data arrays have the same naming abbreviations, but different extension: (`??*****[m|w].swp`). Suffix 'm' stands for full-window output, suffix 'w' denotes subwindow output. In the data files, one row is for one ξ -layer or sub-layer. Columns correspond to different transverse coordinates.

colormaps-full, *multichoice* (""): A list of quantities to output in the full window

colormaps-subwindow, *multichoice* (""): A list of quantities to output in the subwindow

Full window means the **drawn-portion** of the whole simulation window, the area of size $\xi_{\max} \times r_{\max} \eta_{\text{draw}}$.

Subwindow size and location are controlled manually. Output of the following quantities is possible:

'Er': first transverse component of the electric field, E_r or E_x	(er***** [w] .png)
'Ef': second transverse component of the electric field, E_φ or E_y	(ef***** [w] .png)
'Ez': z -component of the electric field, E_z	(ez***** [w] .png)
'Phi': wakefield potential, Φ	(fi***** [w] .png)
'Bf': φ or y component of the magnetic field, B_φ or B_y	(bf***** [w] .png)
'Bz': perturbation of the longitudinal magnetic field, $B_z - B_0$	(bz***** [w] .png)
'pr': first transverse component of the electron momentum, p_{er} or p_{ex}	(pr***** [w] .png)
'pf': second transverse component of the electron momentum, $p_{e\varphi}$ or p_{ey}	(pf***** [w] .png)
'pz': z -component of the electron momentum, p_{ez}	(pz***** [w] .png)
'pri': first transverse component of the ion momentum, p_{ir} or p_{ix}	(ir***** [w] .png)
'pfi': second transverse component of the ion momentum, $p_{i\varphi}$ or p_{iy}	(if***** [w] .png)
'pzi': z -component of the ion momentum, p_{iz}	(iz***** [w] .png)
'nb': charge density of particle beams, ρ_b	(nb***** [w] .png)
'ne': perturbation of the plasma electron density, $n_e - 1$	(ne***** [w] .png)
'ni': perturbation of the plasma ion density, $n_i - 1$	(ni***** [w] .png)
'Sf': z -component of the total energy flux density (e.f.d.), S_z	(sf***** [w] .png)
'Sr': r -component of the total e.f.d., S_r	(sr***** [w] .png)
'dS': z -component of the thermal e.f.d., $S_z - S_{fz}$	(sd***** [w] .png)
'Sf2': r -weighted z -component of the total e.f.d., $2\pi r S_z$	(2f***** [w] .png)
'Sr2': r -weighted r -component of the total e.f.d., $2\pi r S_r$	(2r***** [w] .png)
'dS2': r -weighted z -component of the thermal e.f.d., $2\pi r(S_z - S_{fz})$	(2d***** [w] .png)
'Wf': total energy density, W	(wf***** [w] .png)
'dW': thermal energy density, $W - W_f$	(wd***** [w] .png)
'SEB': z -component of the electromagnetic e.f.d., S_{ez}	(se***** [w] .png)
'I1': laser intensity, a^2	(I1***** [w] .png)

If a quantity is undefined (like electron momentum at points of zero electron density), then zero is output at this point.

colormaps-type, *choice* (y): Controls whether functions of (r, ξ) are output as data files or as pictures:

- 'n' or 'numbers': Only data files.
- 'y' or 'pictures': Only pictures.
- 'F' or 'both': Both pictures and data files.

drawn-portion, *float* (1): Fraction of the simulation window to be referred as the full window, η_{draw}

A number between 0 and 1 (Fig. 5a). Used to exclude uninteresting near-wall regions from the output.

subwindow-xi-from, *float* (-5): Right boundary of the subwindow, ξ_{from}

subwindow-xi-to, *float* (-10): Left boundary of the subwindow, ξ_{to}

subwindow-r-from, *float* (0): Bottom boundary of the subwindow, r_{from}

subwindow-r-to, *float* (3): Top boundary of the subwindow, r_{to}

Four parameters controlling the size and position of the subwindow (Fig. 5b).

output-merging-r, *integer* (1): Merging in r , grid points, N_{mr}

output-merging-z, *integer* (1): Merging in ξ , grid points, $N_{m\xi}$

These numbers control output of one average value from several grid points (Fig. 5a). Values from the specified number of grid points (N_{mr} in r and $N_{m\xi}$ in ξ) are added together and divided by the number of points ($N_{mr}N_{m\xi}$). This procedure is made after the passage of the whole simulation window, when all the values are written to an auxiliary file. The subwindow output is not affected by these options.

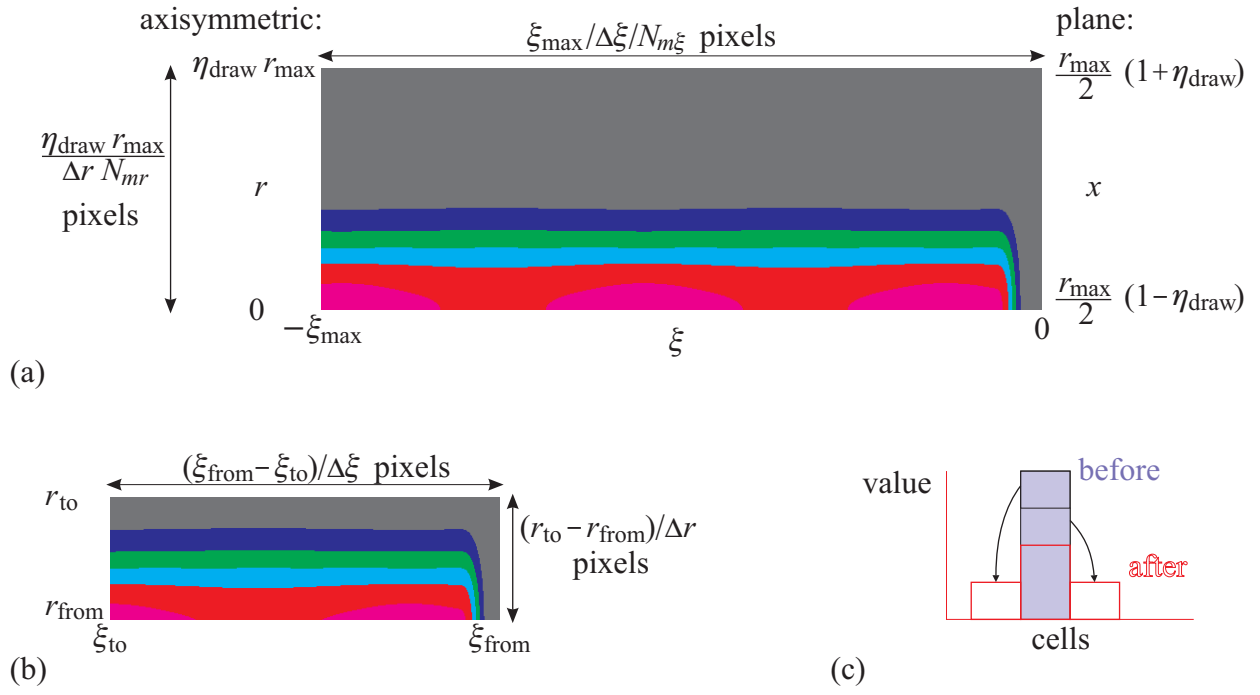


Figure 5: Physical and pixel sizes of the full-window colored map (a) and subwindow colored map (b); elementary smoothing procedure (c).

palette, choice (d): Colormap palette: default/greyscale/hue/bluwhitered

Coloring method used to display values of functions on (r, ξ) plane (Fig. 6):

‘d’ or ‘default’: Distinctly-colored palette

‘g’ or ‘greyscale’: Greyscale palette

‘h’ or ‘hue’: Hue-equidistant palette

‘b’ or ‘bluwhitered’: Blue-white-red palette

Each palette has 8 distinct colors for positive values of quantities and 7 colors for negative values. One color is reserved for regions of zero density at plasma density maps (black for ‘default’ and ‘greyscale’ palettes, pure magenta for ‘hue’, and pure blue for ‘bluwhitered’).

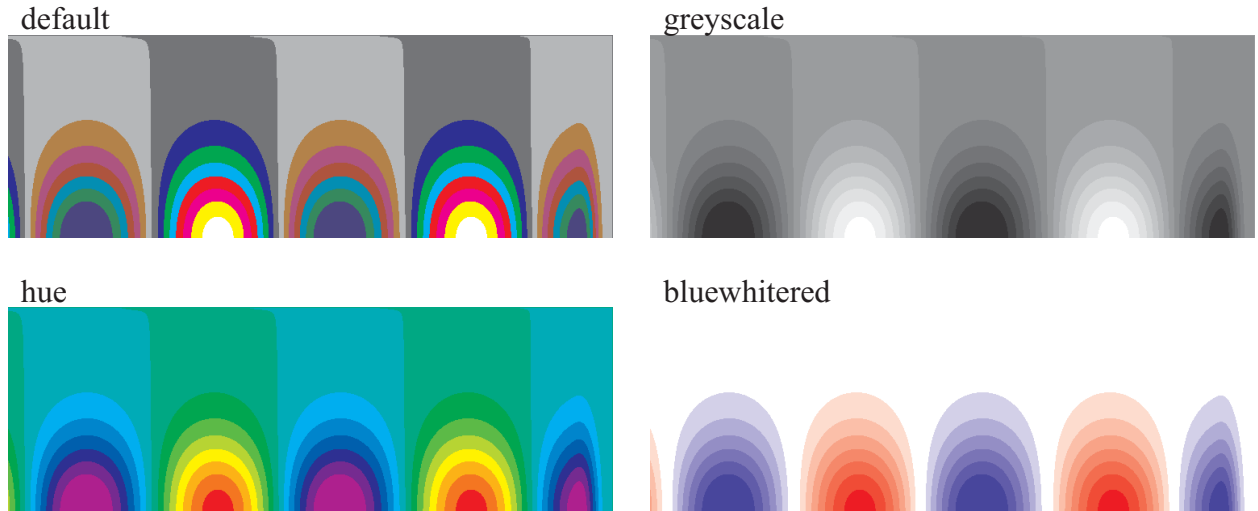


Figure 6: Examples of colormap palettes.

The following parameters (color steps) set up a correspondence between the increment of a quantity and color change on the picture:

E-step, float (0.1): Components of the electric field (‘Er’, ‘Ef’, ‘Ez’).

Phi-step, float (0.1): Wakefield potential (‘Phi’).

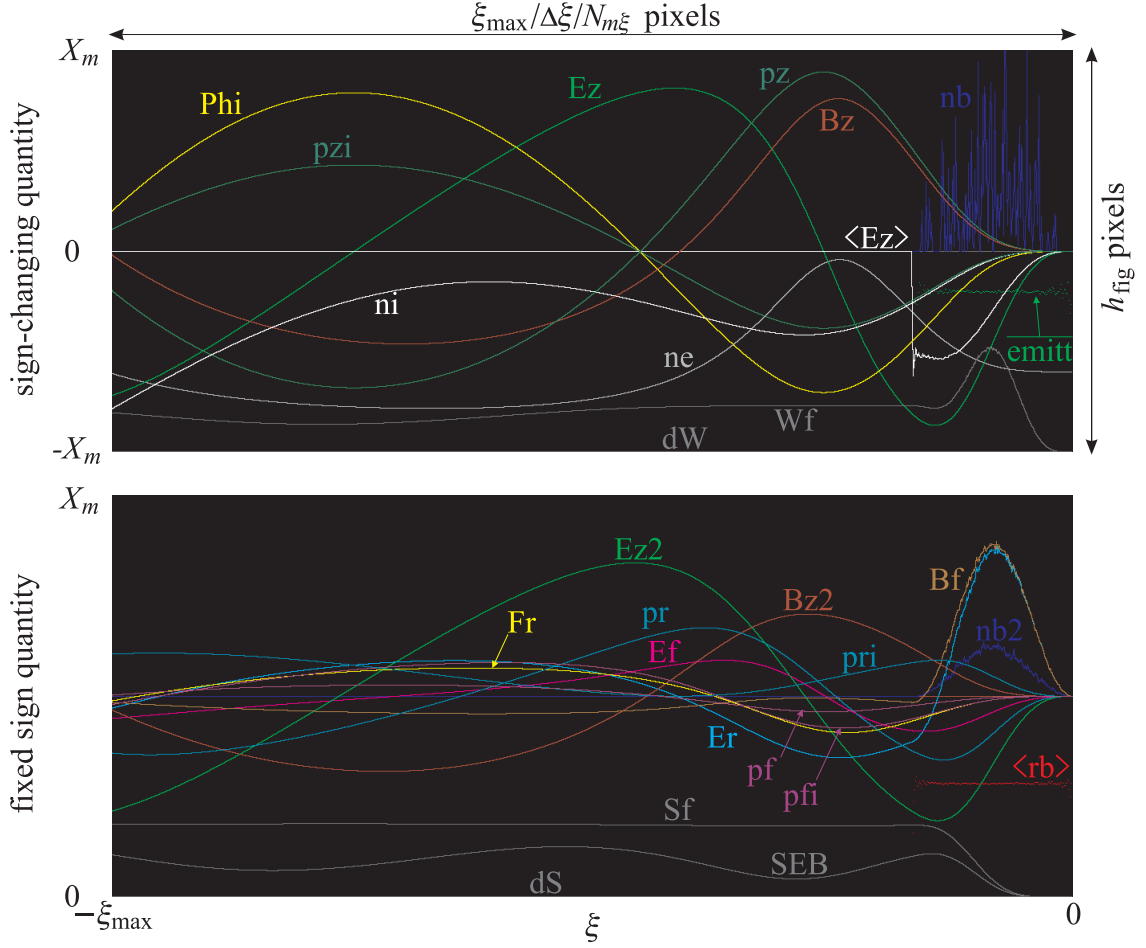


Figure 7: Physical and pixel sizes of the figures showing functions of ξ and colors used for displaying output quantities in the first group (top) and second group (bottom). The exact appearance of colors in the manual may depend on the viewing software.

- Bf-step**, *float* (0.1): Transverse magnetic field ('Bf').
- Bz-step**, *float* (0.1): Longitudinal magnetic field ('Bz').
- electron-momenta-step**, *float* (0.1): Electron momenta ('pr', 'pf', 'pz').
- ion-momenta-step**, *float* (0.1): Ion momenta ('pri', 'pfi', 'pzi').
- nb-step**, *float* (0.1): Charge density of particle beams ('nb').
- ne-step**, *float* (0.1): Density of plasma electrons ('ne').
- ni-step**, *float* (0.01): Density of plasma ions ('ni').
- flux-step**, *float* (0.01): Components of energy flux densities ('Sf', 'Sr', 'dS', 'SEB').
- r-corrected-flux-step**, *float* (0.01): *r*-corrected energy flux densities ('Sf2', 'Sr2', 'dS2').
- energy-step**, *float* (0.01): Energy densities ('Wf', 'dW').

The color step for the laser intensity map ('ll') is always $a_0^2/7$.

5.6.2 Functions of ξ

These keys control output of various quantities as functions of ξ , either in the form of a graph, or in the form of a data array. The graphs are plotted in files named (u****.png) or (v****.png) by different colors (Fig. 7), where (****) is the time of output in the 5-digit representation. The 5-digit representation is the integer part of time or its first five significant digits, if the time is greater than 10^6 . The exact time and its 5-digit representation are appended to file (times.dat). Corresponding data is scattered around (xi_pre.****.swp), where pre is a prefix for a physical quantity. Each file contains a single column with quantity values. The corresponding xi values are written to (xi_****.swp).

f(xi), *multichoice* (Ez,nb2,Ez2,dS,Sf,SEB): A list of quantities to output as functions of ξ .

The quantities can be listed in an arbitrary order. There are two groups of quantities, which differ by the picture they are plotted on. Indicated in braces are: the column number in the substepped data array (**?*****.det**) (Sec. 5.6.6), the color and style of the graph in (**?*****.png**).

First group:				(u*****.png)
'ne'	{2, grey line}	$n_e(r_{ax})$	on-axis density of plasma electrons	(xi_ne_*****.swp)
'nb'	{3, blue line}	$\rho_b(r_{ax})$	on-axis charge density of the beam	(xi_nb_*****.swp)
'Ez'	{4, green line}	$E_z(r_{ax})$	on-axis z -component of the electric field	(xi_Ez_*****.swp)
'Eza'	{5, white line}	E_{az}	average longitudinal electric field acting on the beam slice	(xi_Eza_*****.swp)
'Bz'	{6, dark red line}	$B_z(r_{ax}) - B_0$	on-axis z -component of the magnetic field	(xi_Bz_*****.swp)
'Phi'	{7, yellow line}	$\Phi(r_{ax})$	on-axis wakefield potential	(xi_Phi_*****.swp)
'pz'	{8, dark green line}	$p_{ez}(r_{ax})$	on-axis z -momentum of plasma electrons	(xi_pz_*****.swp)
'em'	{9, green points}	ϵ	emittance of the beam slice	(xi_em_*****.swp)
'dW'	{10, dark grey line}	dW_{int}	thermal energy per unit length	(xi_dW_*****.swp)
'Wf'	{11, dark grey line}	W_{int}	total energy per unit length	(xi_Wf_*****.swp)
'ni'	{12, white line}	$n_i(r_{ax})$	on-axis density of plasma ions	(xi_ni_*****.swp)
'pzi'	{13, dark green line}	$p_{iz}(r_{ax})$	on-axis z -momentum of plasma ions	(xi_pzi_*****.swp)
Second group:				(v*****.png)
'nb2'	{2, blue line}	$\rho_b(r_{aux})$	off-axis charge density of the beam	(xi_nb2_*****.swp)
'Er'	{3, cyan line}	E_r or $E_x(r_{aux})$	off-axis transverse electric field	(xi_Er_*****.swp)
'Ez2'	{4, green line}	$E_z(r_{aux})$	off-axis longitudinal electric field	(xi_Ez2_*****.swp)
'Bf'	{5, brown line}	B_φ or $B_y(r_{aux})$	off-axis φ - or y component of the magnetic field	(xi_Bf_*****.swp)
'Bz2'	{6, dark red line}	$B_z(r_{aux}) - B_0$	off-axis z -component of the magnetic field	(xi_Bz2_*****.swp)
'Fr'	{7, yellow line}		average focusing force, $(\Phi_{aux} - \Phi_{ax})(r_{aux} - r_{ax})$	(xi_Fr_*****.swp)
'pr'	{8, dark blue line}	p_{er} or $p_{ex}(r_{aux})$	off-axis r - or x -momentum of plasma electrons	(xi_pr_*****.swp)
'pf'	{9, violet line}	$p_{e\varphi}$ or $p_{ey}(r_{aux})$	off-axis φ - or y -momentum of plasma electrons	(xi_pf_*****.swp)
'rb'	{10, red points}	R_b or X_b	radius/width of the beam	(xi_rb_*****.swp)
'xb'	{11, dark red points}	0 or X_{b0}	transverse displacement of the beam (enabled by 'rb')	(xi_xb_*****.swp)
'dS'	{12, dark grey line}	$\Psi - \Psi_f$	integral thermal energy flux	(xi_dS_*****.swp)
'Sf'	{13, dark grey line}	Ψ	integral total energy flux	(xi_Sf_*****.swp)
'SEB'	{14, dark grey line}	Ψ_e	integral electromagnetic energy flux	(xi_SEB_*****.swp)
'pri'	{15, dark blue line}	p_{ir} or $p_{ix}(r_{aux})$	off-axis r - or x -momentum of plasma ions	(xi_pri_*****.swp)
'pfi'	{16, violet line}	$p_{i\varphi}$ or $p_{iy}(r_{aux})$	off-axis φ - or y -momentum of plasma ions	(xi_pfi_*****.swp)
'Ef'	{17, magenta line}	E_φ or $E_y(r_{aux})$	off-axis φ - or y component of the electric field	(xi_Ef_*****.swp)
'Sw'	{18, dark grey line}	Ψ_w	integral total energy flux plus wall losses	(xi_Sw_*****.swp)
'll'	{-, cyan line}	$a^2(r_{ax})$	laser intensity on the axis	(xi_ll_*****.swp)

Where emittance ϵ of the beam slice is defined as:

$$\text{generally: } \epsilon^2 = \left\langle (|\vec{r}_b^\perp| - \langle |\vec{r}_b^\perp| \rangle)^2 \right\rangle \left\langle (|\vec{p}_b^\perp| - \langle |\vec{p}_b^\perp| \rangle)^2 \right\rangle - \left\langle (|\vec{r}_b^\perp| - \langle |\vec{r}_b^\perp| \rangle)(|\vec{p}_b^\perp| - \langle |\vec{p}_b^\perp| \rangle) \right\rangle^2,$$

$$\text{cylindrical case: } \epsilon^2 = \langle r_b^2 \rangle \left(\langle p_{br}^2 \rangle + \langle p_{b\varphi}^2 \rangle \right) - \langle r_b p_{br} \rangle^2,$$

$$\text{plane case: } \epsilon^2 = (\langle x_b^2 \rangle - \langle x_b \rangle^2)(\langle p_{bx}^2 \rangle - \langle p_{bx} \rangle^2) - (\langle x_b p_{bx} \rangle - \langle x_b \rangle \langle p_{bx} \rangle)^2.$$

Beam transverse displacement X_{b0} (is nonzero only in the plane geometry) is defined as $X_{b0} = \langle x_b \rangle$.

Beam radius R_b or half-width X_b is defined as: $R_b = \sqrt{\langle r_b^2 \rangle}$ or $X_b = \sqrt{\langle x_b^2 \rangle - X_{b0}^2}$.

The averaging is taken over all beam particles in the layer (the interval of width $\Delta\xi$, **xi-step**).

f(xi)-type, *choice* (n): Output mode for the functions of ξ :

'y' or 'pictures': Only pictures (**u*****.png**) and (**v*****.png**) are created.

'Y' or 'numbers': Only data files (**xi_pre_*****.swp**).

'F' or 'both': Both pictures and data files are created.

'n' or 'n': No output of this kind.

axis-radius, *float* (0): Position of the 'probe' line 1, r_{ax}

auxiliary-radius, *float* (1): Position of the 'probe' line 2, r_{aux}

Two transverse positions at which functions of ξ are output. Both are measured from the geometrical axis (in cylindrical geometry) or middle of the simulation window (in plane geometry). It makes sense to put $r_{ax} \neq 0$ only if the beam goes off-axis (in plane geometry) or if the plasma density is too noisy at the geometrical axis (in cylindrical geometry).

The following parameters (X_m) determine the size of the vertical axis when drawing functions of ξ (Fig. 7). The axis is:

- (0, X_m) for fixed sign quantities,
- ($-X_m$, X_m) for sign-changing quantities.

For ion and electron densities, the axis type depends on X_m :

- if $X_m \geq 1$, then (0, X_m), the absolute value of the density is drawn,
- if $X_m < 1$, then ($-X_m$, X_m), the density perturbation is drawn.

The axis size for the laser intensity ('ll') is always a_0^2 .

E-scale, *float* (1): Most of the fields: 'Er', 'Ef', 'Ez', 'Ez2', '<Ez>', 'Bf', 'Fr'

Phi-scale, *float* (1): Wakefield potential: 'Phi'

Bz-scale, *float* (1): Longitudinal magnetic field: 'Bz', 'Bz2'

electron-momenta-scale, *float* (1): Electron momenta: 'pr', 'pf', 'pz'

ion-momenta-scale, *float* (1): Ion momenta: 'pri', 'pfi', 'pzi'

beam-radius-scale, *float* (5): Beam width and displacement: '<rb>'

nb-scale, *float* (1): Charge density of particle beams: 'nb', 'nb2'

ne-scale, *float* (2): Density of plasma electrons: 'ne'

ni-scale, *float* (1): Density of plasma ions: 'ni'

flux-scale, *float* (1): Integral energy fluxes: 'dS', 'Sf', 'SEB', 'Sw'

energy-scale, *float* (1): Energies per unit length: 'dW', 'Wf'

emittance-scale, *float* (5): Beam emittance: 'em'

5.6.3 Beam particle information as pictures

These keys control output of beam portraits in various parameter spaces. The selected beam macro-particles are drawn as cyan dots in pictures (?*****.png), where (?) shows the content, and (*****) is the time.

output-beam-particles, *multichoice* (""): A list of beam projections to be drawn

Beam macro-particles can be output on the following planes in the following files:

'r': (r, ξ) plane (real space)	(p*****.png)
'pr': (p_{br}, ξ) plane (transverse momentum)	(r*****.png)
'pz': (p_{bz}, ξ) plane (longitudinal phase space)	(z*****.png)
'M': (M_b, ξ) plane (angular momentum)	(m*****.png)

draw-each, *integer* (20): Fraction of beam macro-particles to be drawn, D_b

A beam macro-particle is drawn if its ordinal number is a multiple of D_b .

beam-picture-height, *integer* (300): Height of figures in pixels, h_{fig}

This number determines the vertical size of f(xi) graphs, histograms, and beam portraits except the real space portrait. The latter has the same height as colored maps (equal to $\eta_{\text{draw}} r_{\text{max}} / \Delta r / N_{mr}$).

output-reference-energy, *float* (1000): Reference value for displaying beam momentum, $p_{b,\text{ref}}$.

The following parameters (Y_m) determine the size of the vertical axis for corresponding beam portraits:

beam-pr-scale, *float* (100): Axis is ($-Y_m, Y_m$) for r -momentum of beam particles ('pr')

beam-a-m-scale, *float* (100): Axis is (0, Y_m) for the angular momentum of beam particles ('M')

beam-pz-scale, *float* (2000): Axis for z -momentum of beam particles ('pz')

The latter axis depends on the ratio between Y_m and **output-reference-energy** $p_{b,\text{ref}}$. If $Y_m > p_{b,\text{ref}}$, the axis is (0, Y_m), otherwise it is ($p_{b,\text{ref}} - Y_m, p_{b,\text{ref}} + Y_m$).

5.6.4 Beam information as histograms

These keys control output of beam characteristics in the histogram form, either as a picture (d?*****.png), or as a data file (d?*****.swp), where (?) shows the content, and (*****) is the time. If a macro-particle falls outside the chosen histogram interval, the particle is ignored.

Vertical size of the pictures in pixels is determined by **beam-picture-height** (Fig. 8a). The picture height in physical units equals the highest column. To retain the normalization, the line of 3 values is appended to file (hystog.dat) each time a histogram picture is produced. These values are:

1. Time

2. Histogram type (second character of the filename)
3. Height of the highest column.

The data files for histograms have 2 columns:

1. Number of the cell
2. Number of macro-particles in this cell.

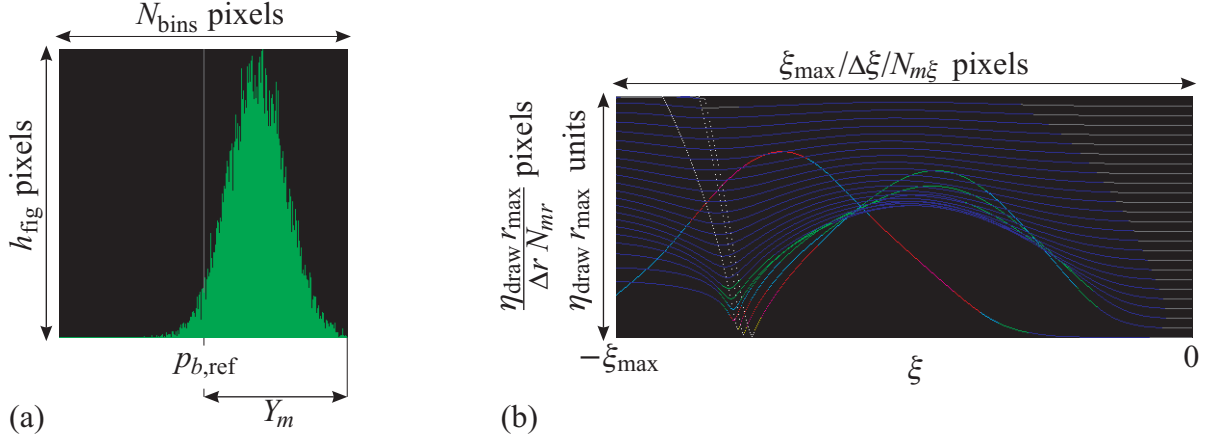


Figure 8: Exemplary histogram of beam longitudinal momentum (a) and trajectories of plasma particles in the blowout regime (b).

histogram-output, *multichoice* (""): Output of various beam properties in the histogram form

Available options, corresponding output quantities, keys determining histogram intervals, and corresponding file names are:

'r':	transverse momentum, p_{br} or p_{bx} , beam-pr-scale ,	(dr*****.png .swp)
'z':	longitudinal momentum, p_{bz} , beam-pz-scale ,	(dz*****.png .swp)
'M':	angular or y -momentum, M_b or p_{by} , beam-a-m-scale ,	(dm*****.png .swp)
'a':	angle between the particle momentum and z -axis, beam-angle-scale ,	(da*****.png .swp)

histogram-output-accel, *multichoice* (""): Output of histograms for accelerated particles only

The same as **histogram output**, but only beam macro-particles with z -momentum greater than **output-reference-energy** are taken into account. Available options, corresponding output quantities, keys determining histogram intervals, and corresponding file names are:

'r':	transverse momentum, p_{br} or p_{bx} , beam-pr-scale ,	(dR*****.png .swp)
'z':	longitudinal momentum, p_{bz} , beam-pz-scale ,	(dZ*****.png .swp)
'M':	angular or y -momentum, M_b or p_{by} , beam-a-m-scale ,	(dM*****.png .swp)
'a':	angle between the particle momentum and z -axis, beam-angle-scale ,	(dA*****.png .swp)

histogram-type, *choice* (y): Mode of the histogram output:

- 'y' or 'pictures': Pictures only,
- 'n' or 'data': Data files only,
- 'F' or 'both': Both pictures and data files.

histogram-bins, *integer* (300): Number of histogram bins (≤ 3000), N_{bins}

beam-angle-scale, *float* (0.1): Axis size for the histogram of beam angular distribution

The axis is from zero to this value.

5.6.5 Trajectories of plasma particles

These diagnostics visualizes trajectories of plasma macro-particles in the simulation window, either as the picture (pp*****.png) (Fig. 8b), or as the data file (*****.pls), where (*****) is the time. The diagnostics works for kinetic plasma models only. Each line of the data file contains 9 values corresponding to one position of one macro-particle:

1. Current ξ -coordinate

2. Number of the macro-particle
3. Transverse coordinate (r or x)
- 4-6. r -, φ -, and z -components of the particle momentum
7. Mass of the macro-particle
8. Charge-to-mass ratio
9. Relativistic factor

trajectories-draw, *choice* (n): Output mode for trajectories of plasma particles:

‘n’ or ‘n’: No output.

‘y’ or ‘y’: Picture mode. Trajectories of chosen plasma macro-particles on (r, ξ) plane are shown by dotted lines with a specified interval in ξ between dots. The dot color represents the gamma-factor γ of the particle. Sizes of the picture are the same as for full-window colored maps.

“Y” or “Y”: Data mode. Information about chosen macro-particles is written to the data file with a specified interval in ξ between successive outputs.

‘F’ or ‘F’: Both picture and data file.

trajectories-each, *integer* (10): Fraction of plasma macro-particles to output

A trajectory of a plasma macro-particle can be drawn or written if the ordinal number of the macro-particle is a multiple of this number.

trajectories-spacing, *integer* (10): Spacing in ξ for consecutive output of macro-particle parameters

This interval is measured in units of the grid step $\Delta\xi$.

trajectories-min-energy, *float* (1): Minimum relativistic factor γ for the particle to be drawn, γ_{\min}

Particles with smaller relativistic factors are ignored. This is useful if you want to exclude weakly perturbed plasma regions from the output.

trajectories-energy-step, *float* (0.5): Color step for visualization of particle energies, C_{step}

The dot color in pictures is determined by $N_{\text{col}} = (\gamma - \gamma_{\min})/C_{\text{step}}$. The order of colors is the same as for the default palette of colored maps.

5.6.6 Detailed (substepped) plasma response

These keys control output of various plasma characteristics at a reduced ξ -step. The longitudinal subwindow for the output is the same as for subwindow colored maps (**subwindow-xi-from**, **subwindow-xi-to**, Sec. 5.6.1).

substepping-output-depth, *integer* (4): Substepping depth for the output (0..4)

How deep sub-stepping in ξ is included into the following output.

substepping-output-map, *y/n* (n): Substepped output of functions of (r, ξ)

If this option is enabled, then quantities chosen in **colormaps-subwindow** are also output with a reduced ξ -step into data files named (??*****.det), where (??) is the two-character quantity abbreviation, and (*****) is the time. The subwindow for the output is the same as for subwindow colored maps. No merging of values is made. If this diagnostics is on, the file (xi*****.det) is also created, which has the same number of lines as data files and contains corresponding values of ξ , one value per line.

substepping-output-f(xi), *y/n* (n): Substepped output of functions of ξ

If enabled, then quantities chosen in **f(xi)** are also output with a reduced ξ -step into data files named (u*****.det) and (v*****.det), where (*****) is the time. The file consists of several columns for numbers. The first column indicates ξ position, for the meaning of the other columns refer to the **f(xi)** option description.

substepping-output-particles, *y/n* (n): Substepped output of plasma particles

If enabled, information about plasma macro-particles is written to data file at each ξ -step or sub-step of the depth specified by **substepping-output-depth**. Particle filtering criteria imposed by **trajectories-each** and **trajectories-min-energy** are applicable.

substepping-output-particles-area, *choice* (f): Area for substepped output of plasma particles:

- 'n' or 'no': The output window is the same as for colored maps. Particle parameters are written to file (*******.pls**), where (*********) is the time.
- 'y' or 'yes': The output window is the same as subwindow for colored maps. Particle parameters are written to file (**s*****.pls**), where (*********) is the time. The file format is the same as for (*******.pls**).

5.7 Saving run state

The following options control periodical savings of the run state.

saving-period, *float* (1000): Time interval between run saves

The run is saved if the time t differs from a multiple of the saving period by less than $\Delta t/2$. Saving is made after completion of the ξ -cycle and drawing all pictures.

save-beam, *y/n* (n): Saving the beam state

The state of the beam is saved in binary file (**tb*****.swp**). The format of the file is the same as that of (**beamfile.bin**). Option works for non-rigid beams only. Independently on this key, the beam state is also saved to (**beamfile.bin**) on reaching the time limit t_{\max} or after manual interruption of the run (by the dot), so that the run can be continued without data loss.

save-plasma, *y/n* (n): Saving the plasma state

The plasma state at the end of the simulation window is saved to files (**pl*****.swp**) (plasma particles) and (**fl*****.swp**) (electric and magnetic fields). Formats of the files are the same as those of (**plasma.bin**) and (**fields.bin**) (Sec. 7.3, 7.4). Option works for kinetic plasma models only. Independently on this key, in regimes with plasma continuation the final plasma state is saved to (**plasma.bin**) and (**fields.bin**) on reaching the time limit t_{\max} or after manual interruption of the run (by the dot), so that the run can be continued without data loss.

The run can be resumed from any saved time ********* by changing the content of (**beamfile.bit**) to *********, renaming (**tb*****.swp**) to (**beamfile.bin**), and, if necessary, renaming (**pl*****.swp**) to (**plasma.bin**) and (**fl*****.swp**) to (**fields.bin**). Any changes in code options (e.g., changes of diagnostics) will take effect on the resumed run.

5.8 Performance

max-ram-megabytes, *integer* (512): Allowed RAM usage for storing the beam, MB

This option defines the amount of RAM in megabytes that LCODE is allowed to use for storing the beam particles. This option is only useful for single-process calculations and is ignored for MPI-enabled version with more than one process. Set to zero if you don't want to store the beam particles in RAM; but keep in mind that it can result in performance loss and excessive disk usage. Note that setting the value too high may result in disabling this feature. In this case you should lower the value or set it to zero. Note that if it is set to a non-zero value that is not large enough to store the particle beam, LCODE will crash during the first time step of the computation. In this case you should increase the value or set it to zero.

5.9 Logging preferences

log-stdout-level, *choice* (d): Verbosity level for printing messages

log-file-level, *choice* (w): Verbosity level for logging to a file:

- "e" or "error": Output error messages only
- "w" or "warning": Output error and warning messages
- "i" or "info": Output error, warning and info messages
- "d" or "debug": Output error, warning, info and debug messages

log-filename, *string* ("lcode.log"): Name of the file to log to

log-file-clean, *y/n* (y): Remove empty log file

If enabled, then empty log files are automatically removed at the end of the run, if any.

save-config, *y/n* (*y*): Enable saving config to a file

save-config-filename, *string* ("lcode.runas.cfg"): Name of the file to save the current config to

This config includes the final version of all parameters, including those set by command-line switches. This may become useful in later debugging, for exact replication of the execution process, and especially after config recovery, as it reflects the automatic changes introduced by the recovery process.

5.10 Miscellaneous options

expected-commit-hash, *string* (""): Commit hash of the expected LCODE version

In case LCODE is executed with this option set to a commit hash, LCODE will warn user when its version differs from the expected one. If **save-config** option is enabled and **expected-commit-hash** is empty, LCODE will dump its built-in commit hash to **save-config-filename**.

6 Initial beam shape

There are two ways to define the initial distribution of beam particles in the six-dimensional phase space.

The first way is to specify all necessary parameters for each beam macro-particle. For this, information about the macro-particles must be written to the binary file (**beamfile.bin**) by an external program. The initial time must be written to the text file (**beamfile.bit**). The code will read this information as the initial state of the beam.

The second way is to specify macroscopic parameters for individual beam segments. A segment is a beam piece of variable length l_s . The segments follow one by one starting from the beginning of the simulation window (at $\xi = 0$). A description of a segment has the format

parameter1=value1, parameter2=value2, ..., parameterN=valueN

If a parameter definition not followed by comma, then it is considered as the last one in the description of this segment. A description must contain at least one parameter defined. Segment descriptions follow one by one in **beam-profile** or in a separate file which **beam-profile** refers to.

Numerical parameters can be specified in scientific notation (like **1e6**) and postfixed with **PI** or **Pi** which acts like multiplication by 3.1415926.

If a parameter is not explicitly defined in the segment description, then it is assigned the default value. The initial default values are given in the following description. To modify default values for all subsequent segments, a special line prefixed with **'default:'** can be used. This line has the same syntax as segment descriptions, but does not define any segment and only changes the default values of some parameters. Re-definition of default values can be made several times.

6.1 Segment parameters

length, *float* (2PI): Length of the segment, l_s

ampl, *float* (0.5): Maximum current in the segment, I_a

Maximum current for this segment in units of **beam-current** I_{b0} .

xishape, *choice* (c): Dependence of the beam current on the longitudinal coordinate, $I_b(\xi)$

In the following variants, the formulae are applicable in the interval $l_s > \delta\xi > 0$, where $\delta\xi = \xi_s - \xi$, and the segment starts at $\xi_s \leq 0$.

'c' or 'cos': Shifted cosine shape,	$I_b(\xi) = 0.5 I_a I_{b0} (1 - \cos(2\pi\delta\xi/l_s)).$
't' or 't': Linear rise of the current,	$I_b(\xi) = I_a I_{b0} \delta\xi/l_s.$
'T' or 'T': Linear decrease of the current,	$I_b(\xi) = I_a I_{b0} (1 - \delta\xi/l_s).$
'l' or 'l': Constant current,	$I_b(\xi) = I_a I_{b0}.$
'h' or 'half-cos': Rising half-period of the shifted cosine,	$I_b(\xi) = 0.5 I_a I_{b0} (1 - \cos(\pi\delta\xi/l_s)).$
'b' or 'b': Decreasing half-period of the shifted cosine,	$I_b(\xi) = 0.5 I_a I_{b0} (1 + \cos(\pi\delta\xi/l_s)).$
'g' or 'g': Decreasing part of Gaussian function with $\sigma_z = l_s/6$,	$I_b(\xi) = 0.5 I_a I_{b0} \exp(-18 \delta\xi^2/l_s^2).$

radius, *float* (1): Radius of the beam segment, σ_r

energy, *float* (1000): Basic longitudinal momentum of beam particles, p_{b0}

vshift, *float* (0): Transverse displacement of the segment (used in plane geometry only), x_0

rshape, *choice* (g): Initial distribution of beam particles in the transverse phase space

Available options:

‘g’ or ‘gaussian’: Random distribution with the probability density

$$f_{\perp}(r_b, p_{br}, p_{b\varphi}) = \frac{r_b}{2\pi\sigma_r^2\alpha_b^2p_{b0}^2} \exp\left(-\frac{r_b^2}{2\sigma_r^2} - \frac{p_{br}^2 + p_{b\varphi}^2}{2\alpha_b^2p_{b0}^2}\right), \quad (\text{axisymmetric beam}),$$

$$f_{\perp}(x_b, p_{bx}, p_{by}) = \frac{1}{(2\pi)^{3/2}\sigma_r\alpha_b^2p_{b0}^2} \exp\left(-\frac{(x_b - x_0)^2}{2\sigma_r^2} - \frac{p_{bx}^2 + p_{by}^2}{2\alpha_b^2p_{b0}^2}\right), \quad (\text{plane geometry}).$$

Here α_b is the angular spread of the beam slice, and x_b is measured from the central plane. For the Gaussian distribution, the beam current $I_b(\xi)$ and the beam density on the axis $\rho_b(0)$ are related as

$$I_b(\xi) = \frac{\rho_b(0)\sigma_r^2}{2}, \quad (\text{axisymmetric beam}),$$

$$I_b(\xi) = \frac{\rho_b(0)\sigma_r}{2\sqrt{2\pi}}, \quad (\text{plane geometry}).$$

‘r’ or ‘regular’: The distribution with the same probability density as for ‘gaussian’, but with a regular distribution of beam particles. Means nothing for rigid beam mode.

‘c’ or ‘cylinder’: Cylinder-shaped distribution with the probability density

$$f_{\perp}(r_b, p_{br}, p_{b\varphi}) = \frac{r_b}{\pi\sigma_r^2\alpha_b^2p_{b0}^2} \exp\left(-\frac{p_{br}^2 + p_{b\varphi}^2}{2\alpha_b^2p_{b0}^2}\right), \text{ for } r < \sigma_r,$$

$$0 \text{ otherwise.} \quad (42)$$

Also works in plane geometry:

$$f_{\perp}(x_b, p_{bx}, p_{by}) = \frac{\sqrt{\sigma_r^2 - (x_b - x_0)^2}}{\pi^2\sigma_r^2\alpha_b^2p_{b0}^2} \exp\left(-\frac{p_{bx}^2 + p_{by}^2}{2\alpha_b^2p_{b0}^2}\right), \text{ for } -\sigma_r + x_0 < x < \sigma_r + x_0,$$

$$0 \text{ otherwise.} \quad (43)$$

‘b’ or ‘brick’: Brick-shaped distribution with the probability density

$$f_{\perp}(x_b, p_{bx}, p_{by}) = \frac{1}{2\pi\sigma_r\alpha_b^2p_{b0}^2} \exp\left(-\frac{(x_b - x_0)^2}{2\sigma_r^2} - \frac{p_{bx}^2 + p_{by}^2}{2\alpha_b^2p_{b0}^2}\right), \text{ for } -\sigma_r + x_0 < x < \sigma_r + x_0,$$

$$0 \text{ otherwise.} \quad (44)$$

Works in plane geometry only.

angspread, *float* (1e-5): Maximum angular spread in the segment, α_0

angshape, *choice* (1): Dependence of the angular spread on the longitudinal coordinate, $\alpha_b(\xi)$

In the following variants, the formulae are applicable in the interval $l_s > \delta\xi > 0$, where $\delta\xi = \xi_s - \xi$, and the segment starts at $\xi_s < 0$.

‘c’ or ‘cos’: Shifted cosine,	$\alpha_b(\xi) = 0.5 \alpha_0 (1 - \cos(2\pi\delta\xi/l_s)).$
‘t’ or ‘t’: Linear rise,	$\alpha_b(\xi) = \alpha_0 \delta\xi/l_s.$
‘T’ or ‘T’: Linear decrease,	$\alpha_b(\xi) = \alpha_0 (1 - \delta\xi/l_s).$
‘l’ or ‘l’: Constant,	$\alpha_b(\xi) = \alpha_0.$
‘h’ or ‘half-cos’: Rising half-period of the shifted cosine,	$\alpha_b(\xi) = 0.5 \alpha_0 (1 - \cos(\pi\delta\xi/l_s)).$
‘b’ or ‘b’: Decreasing half-period of the shifted cosine,	$\alpha_b(\xi) = 0.5 \alpha_0 (1 + \cos(\pi\delta\xi/l_s)).$
‘g’ or ‘g’: Decreasing part of Gaussian function,	$\alpha_b(\xi) = 0.5 \alpha_0 \exp(-18 \delta\xi^2/l_s^2).$

espread, *float* (0): Auxiliary value of the longitudinal momentum, p_a

eshape, *choice* (m): Longitudinal momentum distribution of beam particles, $f_{\parallel}(p_{bz})$

Available options:

‘m’ or ‘monoenergetic’: Monoenergetic,	$f_{\parallel}(p_{bz}) = \delta(p_{bz} - p_{b0}).$
‘u’ or ‘uniform’: Uniform over the interval,	$f_{\parallel}(p_{bz}) = (p_{b0} - p_a)^{-1}$ if $p_{b0} > p_{bz} > p_a,$ $f_{\parallel}(p_{bz}) = 0$ otherwise.
‘l’ or ‘linear’: Linear energy growth from p_a to p_{b0} ,	$f_{\parallel}(p_{bz}) = \delta(p_{bz} - p_{b0} \delta\xi/l_s - p_a(1 - \delta\xi/l_s)).$
‘g’ or ‘gaussian’: Gaussian distribution,	$f_{\parallel}(p_{bz}) = \frac{e^{-(p_{bz} - p_{b0})^2/(2p_a^2)}}{\sqrt{2\pi}p_a}$
‘N’ or ‘N’: N monoenergetic fractions (N is a digit, 2 ... 9),	$f_{\parallel}(p_{bz}) = \sum_{i=0}^{N-1} \delta(p_{bz} - p_i), \quad p_i = p_a + \frac{i}{N-1}(p_{b0} - p_a)$

m/q, *float* (1): Absolute value of mass-to-charge ratio, compared to the electron

6.2 Example of a beam profile

```
default: angspread=3e-3, energy=2000
xishape=cos, ampl=1, length=6PI
```

The first line redefines the default values for two options.

The second line defines the beam segment of the length 6π , current $I_b(\xi) = 0.5 I_{b0}(1 - \cos(|\xi|/3))$, and Gaussian transverse distribution (hardcoded default value) with $\sigma_r = 1$ (hardcoded default value) and $\alpha_b = 0.003$ (hardcoded default ξ -dependence, new default value). All particle in the segment have the same longitudinal momentum (hardcoded default distribution) that equals 2000 (new default value). Particles are either electrons or positrons, depending on the sign of I_{b0} .

7 Format of other input and output files

7.1 beamfile.bin

This file contains information about beam macro-particles in the binary form. For each particle, 8 values are written, 8 bytes each (type double). These values are:

1. Longitudinal position, ξ_b .
2. Transverse position, r_b (cylindrical geometry) or x_b (plane geometry).
3. Longitudinal momentum, p_{bz} .
4. Transverse momentum, p_{br} (cylindrical geometry) or p_{bx} (plane geometry).
5. Angular momentum M_b (cylindrical geometry) or third momentum component p_{by} (plane geometry).
6. Absolute value of the charge-to-mass ratio, compared to electron.
7. Charge carried by the macro-particle. The charge unit is $\Delta\xi mc^2/(2e)$.
8. Ordinal number of the macro-particle.

As follows from the data format, the actual beam charge depends on the dimensionless longitudinal grid step **xi-step**. If the beam generated with some $\Delta\xi$ is used in a continuation run with different $\Delta\xi$, then the beam

density seen by the code will differ from the original one by the ratio of grid steps.

The last macro-particle in (`beamfile.bin`) always has $\xi_b = -100000.0$ and serves as the end-of-file sign.

7.2 `beamfile.bit`

Contains the current time (a decimal number in the text form) and serves as the indicator of the continuation mode. If this file is present, the code tries to continue a previous run.

7.3 `plasma.bin`

File (`plasma.bin`) contains information about plasma macro-particles (one line for one macro-particle). It has 6 columns:

1. Transverse coordinate of the macro-particle (r or x) counted from the bottom of the simulation window.
2. First component of the transverse momentum (p_r or p_x) of the macro-particle (not of a single electron or ion). It equals the particle velocity times relativistic factor times “mass” of the macro-particle.
3. Second component of the transverse momentum (p_φ or p_y) of the macro-particle.
4. Longitudinal momentum (p_z) of the macro-particle.
5. “Mass” of the macro-particle. For uniform electrons of the unit density (i.e., of the density n_0), the “mass” is just the cross-section corresponding to this macro-particle (it is a ring in the cylindrical geometry or a rectangle in the plane geometry). For heavier particles, the “mass” is correspondingly greater.
6. “Charge” of the macro-particle. It is the “mass” times the real charge-to-mass ratio for particles of this sort.

When the run is normally terminated or interrupted in the regimes of a long plasma, the final parameters of all macro-particles are automatically saved to (`plasma.bin`). If the run is then continued, the initial plasma parameters are taken from (`plasma.bin`). The same happens if a new run is started with an arbitrary initial plasma profile.

7.4 `fields.bin`

File (`fields.bin`) contains information about the fields and plasma currents. Each line in (`fields.bin`) corresponds to a grid point. Number of lines is $N_r + 1$ (number of grid steps plus one). Each line contains 8 values:

$E_r, E_\varphi, E_z, B_\varphi, B_z, p_r, p_\varphi, p_z$ for cylindrical geometry and fluid plasma model,
 $E_x, E_y, E_z, B_y, B_z, p_x, p_y, p_z$ for plane geometry and fluid plasma model,
 $E_r, E_\varphi, E_z, B_\varphi, B_z, j_r, j_\varphi, j_z$ for cylindrical geometry and kinetic plasma model,
 $E_x, E_y, E_z, B_y, B_z, j_x, j_y, j_z$ for plane geometry and kinetic plasma model.

Here p_α are components of the electron momentum; j_α are components of the total current density.

When the run is normally terminated or interrupted in the regimes of a long plasma, the final fields are automatically saved to (`fields.bin`). For kinetic plasma models, the run can be then continued with the initial fields taken from (`plasma.bin`). The same happens if a new run is started with an arbitrary initial plasma profile.

7.5 Laser files `ls???????.???swp`

This file contains information about real and imaginary parts of the laser envelope a in the binary form, layer-by-layer, towards decreasing ξ . First, $N_r + 1$ values are written for the real part, in the order of increasing r (or x), then the same for the imaginary part.

7.6 `r*****.det`

This file contains auxiliary information for subwindow diagnostics (Sec. 5.6.1, 5.6.6). If any sub-window diagnostics is on, then 3 values are written (not appended) to file (`f*****.det`), where (`*****`) is the time:

1. Transverse grid step.
2. Lower boundary of the sub-window.
3. Number of ξ -steps inside the sub-window.

7.7 times.dat

This file relates exact times of diagnostic outputs and their 5-digit representations. A line of two values is appended to (`times.dat`) on each output of functions of ξ (Sec. 5.6.2):

1. The integer used in the file name;
2. The corresponding time.

7.8 Diagnostics files

These files are generated by diagnostic tools described in corresponding sections of the manual, and their format is explained on the following pages:

File name	Section	Page	File name	Section	Page
(<code>beamlost.dat</code>)	5.5	19	(<code>captured.pls</code>)	5.5	18
(<code>elocf.dat</code>)	5.5	18	(<code>s*****.pls</code>)	5.6.6	25
(<code>emaxf.dat</code>)	5.5	18	(<code>*****.pls</code>)	5.6.5	25
(<code>glocf.dat</code>)	5.5	18	(<code>??*****m.swp</code>)	5.6.1	19
(<code>gmaxf.dat</code>)	5.5	18	(<code>??*****w.swp</code>)	5.6.1	19
(<code>hystog.dat</code>)	5.6.4	24	(<code>d?*****.swp</code>)	5.6.4	25
(<code>plzshape.dat</code>)	5.4.1	17	(<code>fl*****.swp</code>)	5.7	31
(<code>??*****.det</code>)	5.6.6	19	(<code>partic.swp</code>)	5.5	19
(<code>u*****.det</code>)	5.6.6	26	(<code>pl*****.swp</code>)	5.7	31
(<code>v*****.det</code>)	5.6.6	26	(<code>tb*****.swp</code>)	5.7	30
(<code>xi*****.det</code>)	5.6.6	26			

7.9 Temporary files

Files (`aver.swp`), (`digcol.swp`), (`digcol2.swp`), (`bfile.swp`), (`info.swp`), (`??*****.swp`) are temporary files and are always deleted in normal regimes

8 Tools built into LCODE

Working with files in `beamfile.bin` format (see 7.1) is complicated due to the fact that the format is binary-based. Frequent tasks like joining two beamfiles, for example to inject probe particles into the beam, are also complicated by this fact. When analyzing the result it's often desirable to work with plain-text decimal data. Though most of the general-purpose programming languages and most of the mathematical software supports working with such array-like files, LCODE allows performing some of the most common operations without the need of external tools.

8.1 Beamfile composition/manipulation

beamfile-compose, *string* (""): Create a beamfile from other beamfiles

In case LCODE was executed with this option set to a filename, it doesn't enter the regular calculations mode. It creates a file with a specified filename by concatenating files, which names were specified in **beamfile-compose-from** and optionally sorting the result. The terminating stub particles of the input files do not make it into the resulting file and the new file is terminated with a newly created one.

Usage example:

```
lcode.exe --beamfile-compose=newbm.bin --beamfile-compose-from=bm1.bin,bm2.bin  
--beamfile-compose-sort=x
```

Create a file (`newbm.bin`) by combining (`bm1.bin`) with (`bm2.bin`) and sorting the particles (Windows).

It's advised to inspect the resulting beamfile (see section 8.2) at all times.

beamfile-compose-from, *string* (""): Input files for beam concatenation

Comma-separated file names for beamfile concatenation.

beamfile-compose-sort, *choice* (n): Sorting mode for beamfile composition

'n' or 'none': No sorting is performed, simple concatenation

'x' or 'xi': Particles are sorted by their ξ coordinate.

It's advised to inspect the resulting beamfile (see section 8.2).

- beamfile-compose-filter**, *choice* (a): Filtering to apply to beamfile composition
 ‘a’ or ‘all’: No filtering is performed, all particles get written to the resulting file
 ‘p’ or ‘positive’: Only positively charged particles get written to the resulting file
 ‘n’ or ‘negative’: Only negatively charged particles get written to the resulting file
- beamfile-compose-stub**, *choice* (y): Write stub particle
 ‘y’ or ‘yes’: The resulting file gets terminated with a stub particle
 ‘n’ or ‘no’: The resulting file does not get terminated with a stub particle

8.2 Beamfile inspection

- beamfile-inspect**, *string* (“”): Allows inspecting files in beamfile.bin format
 In case LCODE was executed with this option set to a filename, it doesn’t enter the regular calculations mode. This option specifies the file name of the file use for beamfile inspection.
 Usage examples:
`lcode.exe --beamfile-inspect=beamfile.bin`
 Interactively browse the contents of the (`beamfile.bin`) (Windows).
`./lcode --beamfile-inspect=beamfile.bin --beamfile-inspect-mode=d > beamfile.dat`
 Convert the entire (`beamfile.bin`) into decimal form and save the result into a file (`beamfile.dat`) (UNIX).
- beamfile-inspect-mode**, *choice* (n): Sorting mode for beamfile composition:
- ‘i’ or ‘interactive’: Interactive browsing of the beamfile contents. A pager-like program is started that displays decimal data from the file specified and allows scrolling the output buffer. Please refer to the interactive help accessible by pressing the ‘h’ button for instructions about using the interactive mode.
 Note that this mode outputs only up to three significant digits for a nicer preview! For higher precision use the ‘dump’ mode or read the binary data directly from the beamfile.
 - ‘d’ or ‘dump’: Dumps the beamfile contents in decimal form.
 Note that converting the data into decimal form infers a slight precision loss!
 - ‘s’ or ‘stats’: Outputs beamfile statistics. Outputs the amount of the partices contained in the beamfile, the presence and location of the terminated stub particle, the amount of positively and negatively charged particles, the ξ -range, and other facts about the file.